

AD-A273 045



2

NAVAL POSTGRADUATE SCHOOL Monterey, California



SWC
NOV 1 1993

THESIS

ASSESSMENT OF ATMOSPHERIC INFLUENCE
ON SURVEILLANCE RADAR PERFORMANCE
IN LITTORAL ZONES

by

Kyle M. Craigie

September 1993

Thesis Advisor:
Second Reader:

Kenneth L. Davidson
Frederic Levien

Approved for public release; distribution is unlimited.

93 11 23 054

93-28753

DISCLAIMER NOTICE



THIS DOCUMENT IS BEST QUALITY AVAILABLE. THE COPY FURNISHED TO DTIC CONTAINED A SIGNIFICANT NUMBER OF COLOR PAGES WHICH DO NOT REPRODUCE LEGIBLY ON BLACK AND WHITE MICROFICHE.

REPORT DOCUMENTATION PAGE

Form Approved OMB No. 0704

Public reporting burden for this collection of information is estimated to average 1 hour per response, including the time for reviewing instruction, searching existing data sources, gathering and maintaining the data needed, and completing and reviewing the collection of information. Send comments regarding this burden estimate or any other aspect of this collection of information, including suggestions for reducing this burden, to Washington headquarters Services, Directorate for Information Operations and Reports, 1215 Jefferson Davis Highway, Suite 1204, Arlington, VA 22202-4302, and to the Office of Management and Budget, Paperwork Reduction Project (0704-0188) Washington DC 20503.

1. AGENCY USE ONLY (Leave blank)	2. REPORT DATE September 1993	3. REPORT TYPE AND DATES COVERED Master's Thesis
----------------------------------	----------------------------------	---

4. TITLE AND SUBTITLE ASSESSMENT OF ATMOSPHERIC INFLUENCE ON SURVEILLANCE RADAR PERFORMANCE IN LITTORAL ZONES	5. FUNDING NUMBERS
--	--------------------

6. AUTHOR(S) Kyle M. Craigie	
---------------------------------	--

7. PERFORMING ORGANIZATION NAME(S) AND ADDRESS(ES) Naval Postgraduate School Monterey CA 93943-5000	8. PERFORMING ORGANIZATION REPORT NUMBER
---	--

9. SPONSORING/MONITORING AGENCY NAME(S) AND ADDRESS(ES)	10. SPONSORING/MONITORING AGENCY REPORT NUMBER
---	--

11. SUPPLEMENTARY NOTES The views expressed in this thesis are those of the author and do not reflect the official policy or position of the Department of Defense or the U.S. Government.

12a. DISTRIBUTION/AVAILABILITY STATEMENT Approved for public release; distribution is unlimited.	12b. DISTRIBUTION CODE
---	------------------------

13. ABSTRACT (maximum 200 words)
Acoustic sensors, traditionally thought of as the mainstay of modern ASW's means of detection and localization, are rapidly becoming secondary in the littoral zones to active sensors such as radar. The coastal region has a dynamic meteorological environment dominated by surface and near-surface ducts which influence sea clutter. Accurate, timely description of the effects this changing environment has on sensor performance is mandatory for the ASW tactician to utilize his sensors. The Radio Physics Optics (RPO) program and the Engineer's Refractive Effects Prediction System (EREPS) are used to evaluate influence of a measured environment. Both prediction systems are then applied to a Gulf of Oman winter environmental profile with five generic radars operating parameters. EREPS is used to evaluate factors affecting Wallops Flight Facility Space and Ranging Radar (SPANDAR) detected sea clutter in the littoral zone off the United States East Coast.

14. SUBJECT TERMS Evaporation Duct, Sea Clutter, Littoral Zones	15. NUMBER OF PAGES 87
	16. PRICE CODE

17. SECURITY CLASSIFICATION OF REPORT Unclassified	18. SECURITY CLASSIFICATION OF THIS PAGE Unclassified	19. SECURITY CLASSIFICATION OF ABSTRACT Unclassified	20. LIMITATION OF ABSTRACT UL
---	--	---	----------------------------------

Approved for public release; distribution is unlimited.

ASSESSMENT OF ATMOSPHERIC INFLUENCE
ON SURVEILLANCE RADAR PERFORMANCE
IN LITTORAL ZONES

by

Kyle M. Craigie
Lieutenant Commander, United States Navy
B.S., University of North Carolina at Greensboro, 1978

Submitted in partial fulfillment
of the requirements for the degree of

MASTER OF SCIENCE IN SYSTEMS ENGINEERING
(ELECTRONIC WARFARE)
from the

NAVAL POSTGRADUATE SCHOOL
September 1993

Author:

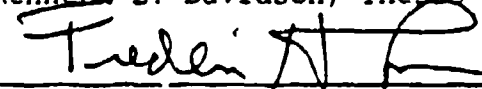


Kyle M. Craigie

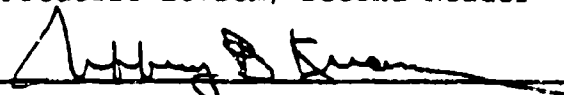
Approved by:



Kenneth L. Davidson, Thesis Advisor



Frederic Levien, Second Reader



Jeffrey B. Knorr, Chairman
Electronic Warfare Academic Group

TABLE OF CONTENTS

I. INTRODUCTION 1

II. COASTAL ENVIRONMENT 3

 A. GENERAL DESCRIPTION 3

 B. TACTICAL CONSIDERATIONS 5

III. ATMOSPHERIC PROPAGATION 6

 A. GENERAL 6

 B. ELECTROMAGNETIC SPECTRUM 7

 C. REFRACTION 9

 1. Subrefraction 12

 2. Super-refraction 12

 3. Trapping 12

 D. DUCTING PHENOMENOM 14

 1. Surface-based Ducts 15

 2. Elevated Ducts 19

 3. Evaporation Ducts 20

 E. SEA CLUTTER 21

 F. IN SITU COLLECTION 22

 1. Shipboard Influences 22

IV. EREPS SEA CLUTTER PREDICTION - MID-ATLANTIC COAST	
SCENARIO	24
A. INTRODUCTION	24
B. CASE 1 - WEAK SURFACE-BASED DUCT AND STRONG	
EVAPORATION DUCT - 1430 15 AUGUST 1990	26
1. Environment	26
2. Radar Performance Analysis	28
a. Radar Observations	28
b. EREPS Prediction	29
C. CASE 2 - STRONG SURFACE-BASED DUCT - 1930 12	
AUGUST 1990	31
1. Environment	31
2. Radar Performance Analysis	33
a. Radar Observations	33
b. EREPS Prediction	34
D. SUMMARY	35
V. COMPARISON OF EFFECT ON DIFFERENT GENERIC SURVEILLANCE	
RADAR SENSORS - GULF OF OMAN	36
A. INTRODUCTION	36
B. GENERIC SURVEILLANCE RADAR SENSOR PARAMETERS	39
C. CASE 3 - 0927/0939L 08 JANUARY 1993 RAWINSONDES	
.	40
1. Environment	40
2. Generic Surveillance Radar Sensor Performance	
Analysis	42

a. Generic Radar - Sensor 1 Analysis . . .	42
b. Generic Radar - Sensor 2 Analysis . . .	45
c. Generic Radar - Sensor 3 Analysis . . .	48
d. Generic Radar - Sensor 4 Analysis . . .	51
e. Generic Radar - Sensor 5 Analysis . . .	56
3. Case 3 Summary	60
 VI. SUMMARY AND RECOMMENDATIONS	 61
 APPENDIX A	 64
A. Attenuation	64
B. Absorption	64
C. Antenna Height	65
 APPENDIX B	 66
A. Engineer's Refractive Effects Prediction System (EREPS)	66
1. Georgia Institute of Technology (GIT) Model	68
B. Integrated Refractive Effects Prediction System (IREPS)	70
C. Radio Physics Optics Program (RPO)	72
 LIST OF REFERENCES	 74
 INITIAL DISTRIBUTION LIST	 75

LIST OF FIGURES

Figure 2.1	Duct created by a sea breeze.	4
Figure 3.1	Electromagnetic Spectrum.	8
Figure 3.2	Refractivity N and Modified Refractivity M Profiles for Standard Atmosphere.	11
Figure 3.3	EM wave paths for various refractive conditions.	14
Figure 3.4	Homogeneous and Non-homogeneous waveguide comparison.	16
Figure 3.5	Surface-based duct.	18
Figure 3.6	Elevated duct.	19
Figure 3.7	Evaporation Duct	20
Figure 4.1	IREPS M-profile for PM 15 August 1990 (Case 1).	27
Figure 4.2	Evaporation duct M-profile using Paulus Model (Case 1).	27
Figure 4.3	SPANDAR PPI Scan for 1430 15 August 1990 (Case 1).	28
Figure 4.4	EREPS loss prediction for 15 AUG 90 (Case 1).	29
Figure 4.5	IREPS M-profile for PM 12 August 1990 (Case 2).	31
Figure 4.6	Evaporation duct M-profile using Paulus Model (Case 2).	32

Figure 4.7 SPANDAR PPI Scan 1930 12 August 1990 (Case 2)	33
Figure 4.8 EREPS loss prediction for PM 12 August 1990 (Case 2)	34
Figure 5.1 Arabian Gulf and Gulf of Oman Map (Case 3).	37
Figure 5.2 IREPS M-profile for 0927 08 JAN 93 (Case 3)	41
Figure 5.3 IREPS M-profile for 0939 08 JAN 93 (Case 3)	41
Figure 5.4 EREPS Sea Clutter prediction for Sensor 1 (Case 3)	43
Figure 5.5 RPO Plot of Sensor 1 0927L 08 JAN 93 (Case 3)	44
Figure 5.6 RPO Plot of Sensor 1 in Standard Atmosphere Conditions (Case 3)	44
Figure 5.7 EREPS Sea Clutter prediction for Sensor 2 (Case 3)	46
Figure 5.8 RPO Plot of Sensor 2 0927L 08 JAN 93 5 (Case 3)	47
Figure 5.9 RPO Plot of Sensor 2 in Standard Atmosphere Conditions (Case 3)	47
Figure 5.10 EREPS Sea Clutter prediction for Sensor 3 (Case 3)	49
Figure 5.11 RPO Plot of Sensor 3 0927L 08 JAN 93 (Case 3)	50

Figure 5.12	RPO Plot of Sensor 3 in Standard Atmosphere Conditions (Case 3).	50
Figure 5.13	EREPS Sea Clutter prediction for Sensor 4 (Case 3).	52
Figure 5.15	RPO Plot of Sensor 4 in Standard Atmosphere Conditions (Case 3).	53
Figure 5.14	RPO Plot of Sensor 4 0927L 08 JAN 93 Looking Seaward (Case 4).	53
Figure 5.16	RPO Plot of Sensor 4 0927L 08 JAN 93 Looking Towards Shore (Case 3).	55
Figure 5.17	EREPS Sea Clutter prediction for Sensor 5 (Case 3).	57
Figure 5.18	RPO Plot of Sensor 5 0927L 08 JAN 93 Looking Seaward (Case 3).	58
Figure 5.19	RPO Plot of Sensor 5 in Standard Atmosphere Conditions (Case 3).	58
Figure 5.20	RPO Plot of Sensor 5 0927L 08 JAN 93 Looking Towards Shore (Case 3).	59

I. INTRODUCTION

The following are selected quotes from the March 1993 Naval Institute Proceedings interview by John F. Morton with VADM. William A. Owens, U. S. Navy, illustrating the current trends and emphasis in ASW. (Morton, 1993, pp.124-129)

The Navy now characterizes itself as an enabling force. The new focus is on littoral warfare...

The Navy appears to be prioritizing both its ASW operational doctrine and its acquisition strategy on what it regards as the main disadvantage of a Third World diesel. To the man, ASW war fighters believe that Third World diesel operators will frequently expose their masts, particularly if the crews are untrained. They will operate at or near periscope depth (down to 200 feet) 50% of the time and possibly more, each time putting the scope up for 10-15 seconds, or if untrained 2-3 minutes. They will snorkel 10% of the time. Quiet operation in shallow water will reduce mobility and constrain operating depth, allowing ASW forces to employ more of their sensing inventory.

ASW is more than just acoustics. The more we have been faced with the challenge of diesel submarines and shallow-water ASW and other new environments, the more we have come to realize the importance of the multi-sensor approach to ASW.

Then, when you can essentially rule out the basins as an operating area for diesel sub, you can concentrate your efforts on the areas surrounding the basin for radar searches by P-3s or S-3s for more traditional active ASW.

Most crucially, the Navy says that Third World diesel operators will have to come to periscope depth "to have a look" at some point prior to or during their attack mode. They are believed incapable of making a submerged approach.

Acoustic sensors, traditionally thought of as the mainstay of modern ASW's means of detection and localization, are

quickly becoming secondary to active sensors such as radar. With the emphasis on radar, we need to be able to exploit its capabilities to the fullest.

A method to maximize a radar system performance is to know the influence of the medium in which it is working, either by direct measurement or through a prediction model. When operating near the surface, the evaporation duct could have profound effects on radar propagation. Sea clutter, backscatter of the radar signal to the receiver from the sea surface, is enhanced by the evaporation duct. This is a major problem for the radar operator trying to detect a submarine in an environment where ducting conditions persist. Such conditions would occur in the Arabian Gulf or Gulf of Oman.

An accurate description of the evaporation duct at any given time usually involves more environmental measurements than time or availability of reliable sensors allow. Therefore, if accurate, easy-to-use prediction systems can be defined, the electromagnetic spectrum user can best utilize his equipment. The purpose of this thesis is to examine the impact of sea clutter and other radar duct effects that exist in the littoral area. The study will incorporate the data/knowledge of duct effects, will evaluate their impact on five generic radar systems and will suggest system/method for detecting diesel submarines in the Gulf of Oman.

II. COASTAL ENVIRONMENT

A. GENERAL DESCRIPTION

As the focus shifts to littoral warfare resulting from the increasing threat from Third World diesel submarines, so must the understanding of the working environment. The atmosphere in the coastal area is usually not homogeneous, either vertically or horizontally. In the coastal environment, anomalous propagation is common due to the land-sea interface. EM ducting conditions are severely impacted by the coastal interface. Due to the abrupt transition that takes place there, surface-based ducts over the ocean do not extend onshore.

One feature of the littoral zone is the land-sea breeze. It is created by a large temperature differential between the land and water causing meso-scale circulation. This differential can be attributed to the over land surface heating during the course of each day compared to the relatively constant temperature over water. The diurnal lateral movement of air is a sea breeze during the day and a land breeze at night.

During the daytime, heated air over land rises aloft and flows outward. At the surface, cool moist air flows on shore. Circulation associated with sea breeze is shown in Figure 2.1.

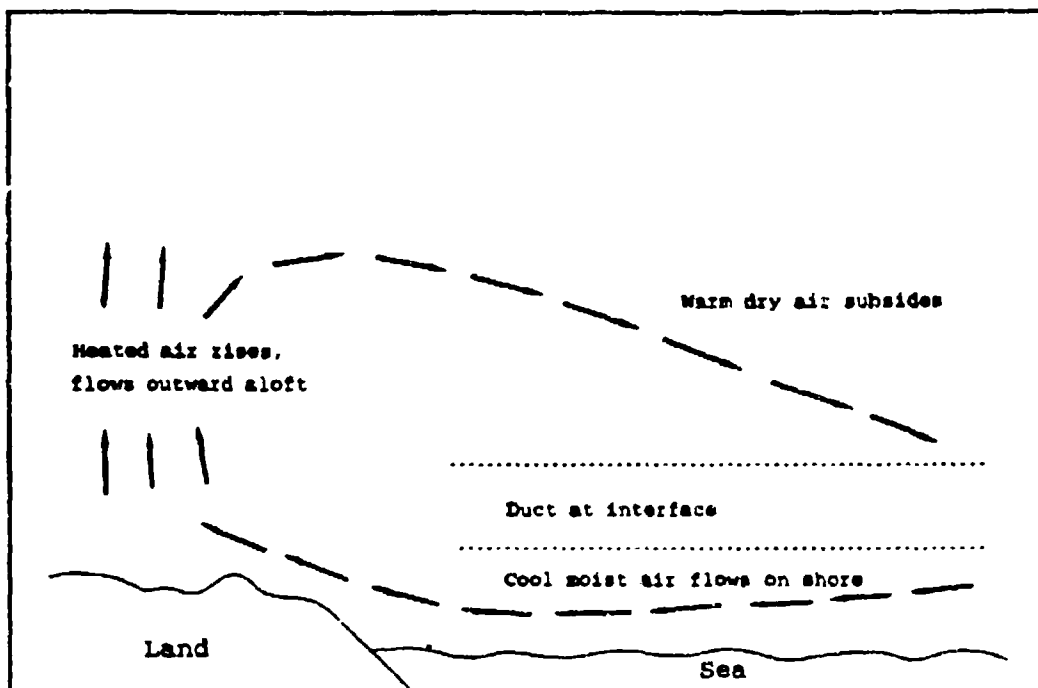


Figure 2.1 Duct created by a sea breeze.

After the marine air crosses the land-sea interface it is heated by the land and begins to flow outward aloft. As it circulates back out to sea, the warm dry air subsides off shore. This sets up the necessary conditions for ducting. Since warm, dry air overlies cool, moist air. Ducting is reduced with mixing. Therefore high winds and ducting are not conducive. Three basic types of ducting result. These are surface-based, evaporative, and elevated which will be discussed later.

D. TACTICAL CONSIDERATIONS

The Third World conventional diesel electric submarine will have a significant amount of operating time at periscope depth to either charge batteries, "to have a look", or simply because low level of training afforded the crew restricts it to this depth. This increases the chance of radar detection.

The existence of ducting conditions in littoral areas works two-fold. Not only does the radar operator enjoy longer ranges, the Electronic Support Measures (ESM) operator will be able to detect a radar's presence to allow time to take evasive actions. Another problem that arises is sea clutter which increases false target detection, but can also mask a low radar cross section target like a periscope.

III. ATMOSPHERIC PROPAGATION

A. GENERAL

In this chapter the electromagnetic spectrum will be discussed followed by a explication of the basics of refraction and an explanation of the trapping and ducting phenomena. Other important factors affecting propagation such as attenuation, absorption and antenna height are discussed in Appendix A.

Electromagnetic waves do not propagate in a straight line while traveling through the atmosphere. The earth's surface and the atmosphere profoundly influence electromagnetic propagation in many ways. The earth's curvature diffracts electromagnetic waves as explained by Huyghens' principle. Huyghen says that every elementary area of a wavefront is a center that radiates in all directions on the front side of the wave front. The earth's surface affects electromagnetic waves as if it were the rough bottom of a lossy wave guide. And lastly, the atmosphere refracts the electromagnetic wave because of its inhomogeneity in index of refraction.

Electromagnetic waves may propagate well beyond normal expected ranges in the anomalous region in the lower atmosphere known as the tropospheric duct. Within this region abnormal propagation can occur either by subrefraction, super-

refraction or by trapping and ducting. Duct formation is associated with a mass of warm, dry air covering a layer of cooler, moist air depicted in Figure 2.1. Typically ducts are one of three basic forms; surface-based, evaporative or elevated. All three and how they are influenced by the coastal region will be discussed later in this chapter.

A standard atmosphere, a non-anomalous propagation medium, would reduce the task of controlling and exploiting the electromagnetic spectrum to a trivial one. However, the actual atmosphere is far more complex, causing electromagnetic wave propagation to be much less predictable. The effects can be greatly extended or diminished ranges, fading, duct trapping and leakage or holes.

B. ELECTROMAGNETIC SPECTRUM

Virtually all modern weapon systems utilize the electromagnetic (EM) spectrum, either actively or passively. Recently EW was brought to the forefront of modern warfare in the Persian Gulf War and with ongoing drug interdiction operations in the Carribean. EM devices are heavily employed in combat systems with their most important role being command and control systems. The single most important factor for today's warfighter is time. Timely, accurate tactical information is critical due to modern stand-off weapon system's high mach numbers and extended ranges.

	(frequency)	300 GHz
	(wavelength)	1 mm
KHF	Radar, space exploration	30 GHz
SHF	Radar, satellite communication	1 cm
UHF	Radar, TV, navigation	3 GHz
		10 cm
VHF	Radar, TV, FM, police, air traffic control	300 MHz
		1 m
HF	SW radio, facsimile, CB	30 MHz
		10 m
MF	AM, marine radio, direction finding	3 MHz
		100 m
LF	Navigation, radio beacon	300 KHz
		1 km
VLF	Navigation, sonar	30 KHz
		10 km
		3 KHz
		100 km

Figure 3.1 Electromagnetic Spectrum.

The EM spectrum includes light, radio waves, x-rays, gamma rays, microwaves, plus many more. Each EM wave differs only in wavelength and frequency, Figure 3.1 illustrates the portion of the spectrum that radar encompasses. The understanding of the medium that EM waves propagate in is absolutely imperative in order to control and exploit its use. EM waves are refracted, or bent, as they propagate through the atmosphere. It is vital to understand the effects of refraction, environmental measurement, and the prediction systems involved.

C. REFRACTION

Refraction occurs due to anomalies caused by the inhomogeneities of the refractive index. Normal atmospheric refraction extends the radar horizon greater than the visual horizon. More often the atmosphere is horizontally homogeneous rather than vertically homogeneous, except as will be shown in the coastal environment.

Refraction refers to the change in direction of travel of an EM wave due to a spatial change in the index of refraction. The index of refraction, (n) , is defined as the ratio of the velocity of a wave in a medium, (v) to its velocity in a vacuum; $n = c/v$. Refraction depends on barometric pressure, temperature, and water vapor pressure.

In the earth's atmosphere, the index of refraction, (n) varies between 1.000250 and 1.000400, in terms of refractivity, or N , defined as:

$$N = (n-1) \times 10^6 \quad (3.1)$$

N may be derived for any altitude from atmospheric pressure, P , the temperature, T , and the partial pressure of water vapor, e , by:

$$N = \frac{(77.6P)}{T} + \frac{(.73 \times 10^5 e)}{T^2} \quad (3.2)$$

where

P = Barometric pressure, mb

e = Water vapor pressure, mb

T = Absolute temperature, K.

In the standard atmosphere refraction decreases as temperature, pressure, and partial pressure of water vapor diminish with an increase in altitude. This is referred to as the refractivity gradient dN/dz ; where z is height. Refractivity's dependence on temperature and relative humidity can be seen in Equation 3.2. As a result of this relationship the EM wave is bent downward at a rate less than the curvature of the earth. For a standard atmosphere N decreases with height at a rate of approximately 39 N/km..

A more useful means of determining regions of ducting is through the atmospheric refractive conditions represented by the modified refractivity index, M . Anomalous conditions occur when refractivity decreases significantly with altitude. The modified refractive index used to describe this case is defined as

$$M = N + 157 z \quad (3.3)$$

where z is height above the earth in km and N is the refractivity at that height. M will increase with height in a standard atmosphere; a positive dM/dz . However, when M

decreases with height a trapping layer is indicated, where the EM wave will be refracted back towards the earth's surface forming a duct. Therefore negative gradients of M make trapping layers easily identifiable indicating a non-standard atmosphere.

The relationship of N and M gradients, Figure 3.2, to refraction for a normal atmosphere are within the following limits; - 79 to 0 N/km and 79 to 157 M/km.

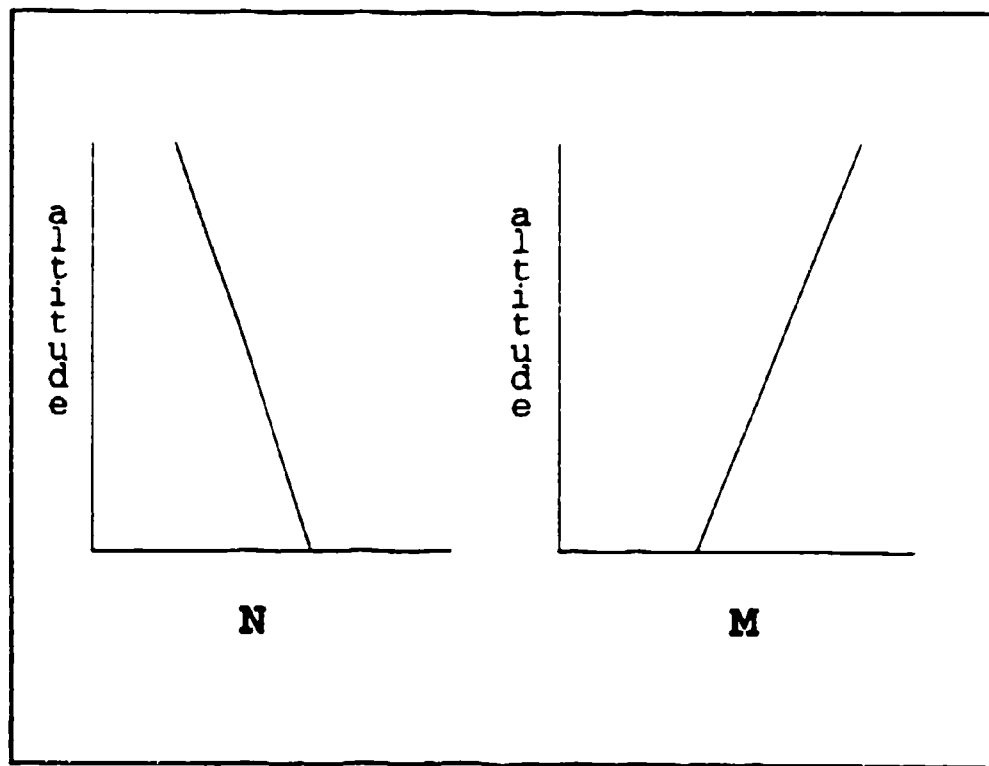


Figure 3.2 Refractivity N and Modified Refractivity M Profiles for Standard Atmosphere.

1. Subrefraction

If temperature and humidity factors result in an increasing value of N with height, the EM wave could bend upward or at least bend downward less than normal. This is known as subrefraction, where $dN/dz > 0$ N/km and $dM/dz > 157$ M/km. The upward bending causes shortened ranges for any system operating within a subrefractive layer. To a radar operating in this region a target will appear to be at greater range and at lower altitude than actual.

2. Super-refraction

If temperature and humidity factors result in a decreasing value of N with height, the EM wave will bend downward more than normal. This condition is known as super-refraction, where dN/dz is -157 to -79 N/km and dM/dz is 0 to 79 M/km. The downward bending results in extended ranges. Now, to a radar operating in this region, unlike subrefraction, the target will appear closer and at a higher altitude than actual.

3. Trapping

When N decreases with altitude at a rate such that $dN/dz < -157$ N/km, much quicker than normal, the EM wave refracts downwards with a curvature equal to or greater than the earth's curvature. Then it will either reflect off the earth's surface or be refracted back upward after entering a region of standard refraction. This is referred to as trapping

because the EM wave is confined to a vertical region and propagates within this region much like a waveguide.

Table 3.1 summarizes the different refractivity gradients and their associated refractive conditions.

	N - Gradient	M - Gradient
Subrefractive	> 0 N/km	> 157 M/km
Normal	-79 to 0 N/km	79 to 157 M/km
Super-refractive	-157 to -79 N/km	0 to 79 M/km
Trapping	< -157 N/km	< 0 M/km

Table 3.1 Conditions of Refractivity

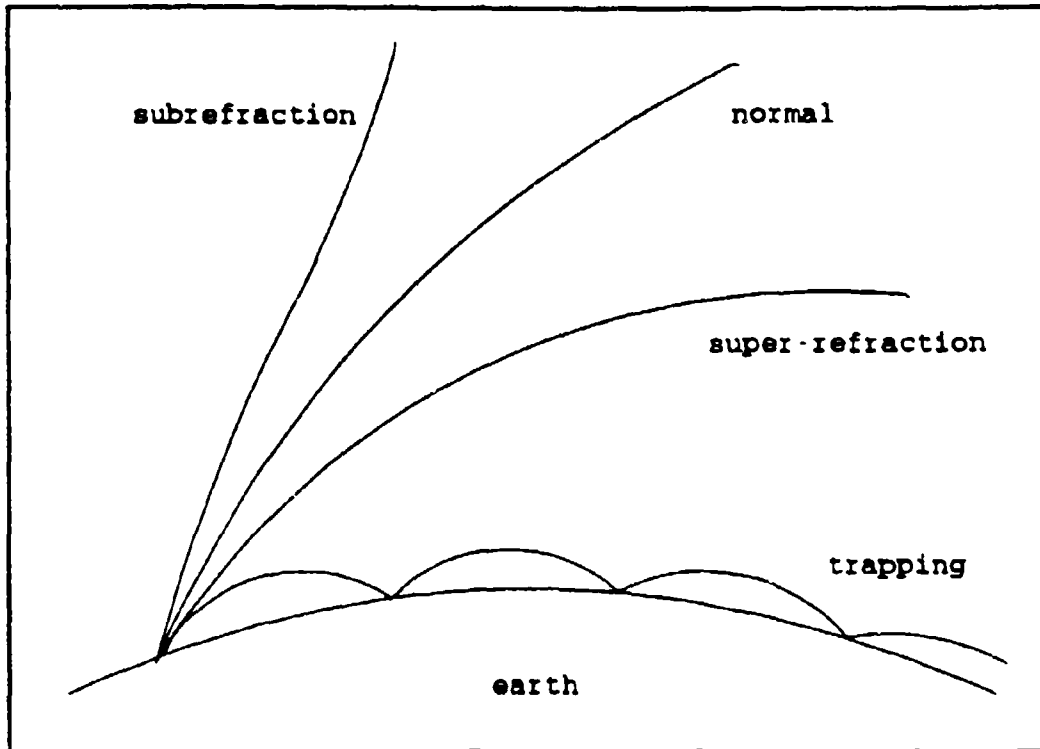


Figure 3.3 EM wave paths for various refractive conditions.

Figure 3.3 illustrates the EM wave paths for various refractive conditions.

D. DUCTING PHENOMENON

A duct can be formed when temperature increases and/or the humidity decreases with height at rapid rate. Temperature increasing with altitude is commonly known as a temperature inversion. Super-refraction is the result of a very steep temperature inversion. This decrease in atmospheric index of refraction with increasing altitude bends the EM wave extending ranges by trapping energy near the earth. A trapping

layer must exist for a duct to form, but the duct may extend above the trapping layer.

The following cases result in the formation of ducts (Sakkas, 1984, pp. 24-25):

1. A temperature inversion at the ground on clear summer nights.

2. A land breeze where warm, dry air moves off the shore above a cooler, moister air over the sea.

3. The temperature inversion as a result of cool air spreading out from the base of a thunder storm in the lowest few thousand feet. Typically lasting no longer than 30 minutes.

4. A subsidence inversion near the ground when the air near the ground is moist. Subsidence is a descending motion of air.

It is apparent from the dynamics of the atmosphere that duct duration is highly variable, anywhere from minutes to hours. A convection mixed atmosphere is not conducive with ducting. Ducting that affects naval EM systems is associated with three distinct types, surfaced-based, evaporative, and elevated ducts.

1. Surface-based Ducts

Surfaced-based ducts occur when the modified refractivity, M increases with altitude in one region and the M value at the top of the trapping layer is less than at the

surface. The EM wave propagates within the duct yielding extended ranges for detection and intercept for frequencies above 100 MHz. Generally, both the transmitter and the receiver antennas should be in the duct.

The surface-based and evaporation ducts are for all purposes, leaky wave guides, or more accurately lossy waveguides. The upper boundary formed by the top of the duct and the bottom by the rough sea surface. An electromagnetic source such as a radar beam sees a duct as a wave guide, but with heavy losses due to either leakage of energy or the

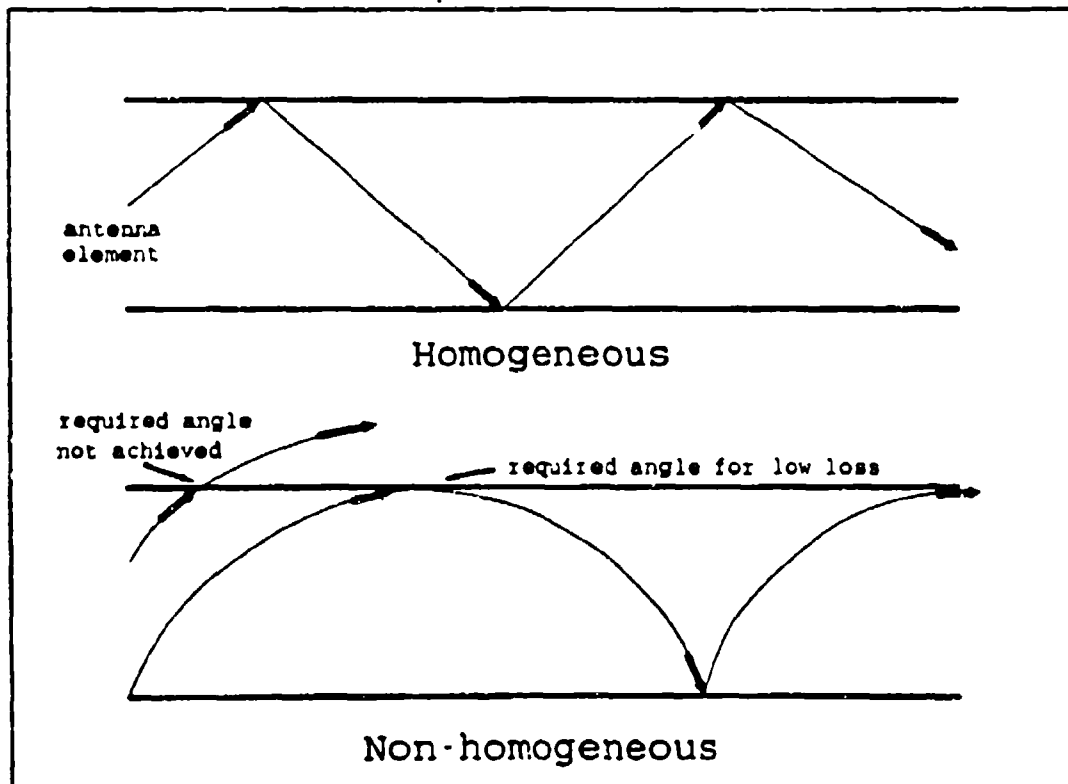


Figure 3.4 Homogeneous and Non-homogeneous waveguide comparison.

conversion of energy to heat caused by the imperfect reflecting boundaries.

The surface-based and evaporation ducts are usually not homogeneous, the index of refraction is constantly changing with distance and altitude. Figure 3.4 illustrates the difference between a homogeneous and nonhomogeneous duct. The homogeneous duct, having smooth boundaries is able to transmit the radar wave with virtually no losses. On the other hand the nonhomogeneous duct, having rough surfaces transmits a radar wave that is undergoing phase changes and energy loss. Leakage at the top boundary occurs when the wave strikes the upper boundary at an angle greater than the critical angle. While changes in phase are induced by irregular surface reflections.

Just like any wave guide, a surface-based duct will not trap and transmit all frequencies. For an EM wave to be channelled, the propagation frequency must be greater than the minimum frequency. The minimum frequency, f_{min} is approximated by:

$$f_{min} = 3.6033 \times 10^{11} d^{-3/2} \quad (3.4)$$

where

f_{min} = minimum frequency, Hz

d = thickness of duct, m.

A critical duct height is easily discerned by rearranging Equation 3.4 as:

$$d_{\min} = \left(\frac{3.6033 \times 10^{11}}{f} \right)^{2/3} \quad (3.5)$$

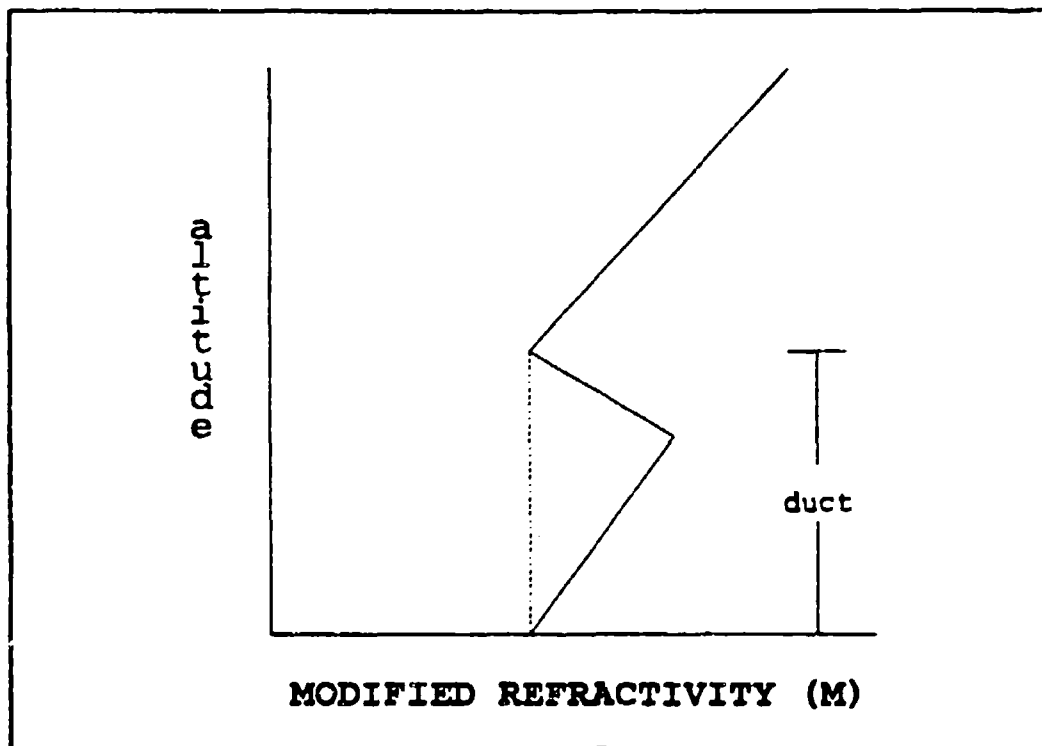


Figure 3.5 Surface-based duct.

2. Elevated Ducts

Elevated ducts are created by the movement of a warm, dry air mass over a cool, moist air mass or by a sinking of air under high pressure centers. The modified refractivity profile, M contains an inflection point above the surface with an M value greater than at the earth's surface, as depicted in Figure 3.6.

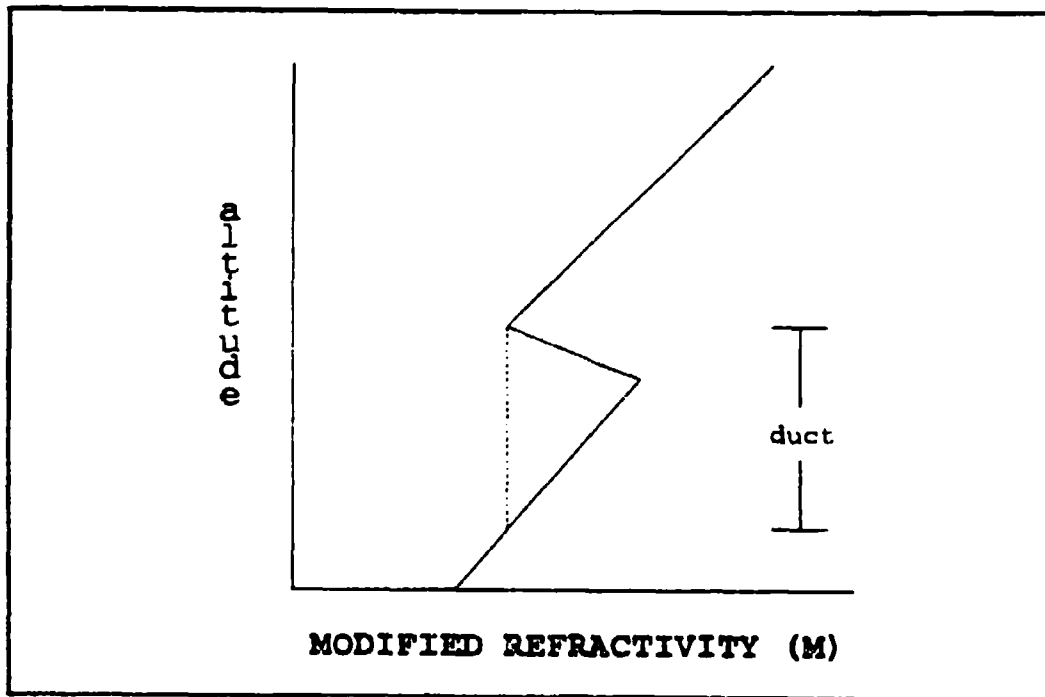


Figure 3.6 Elevated duct.

Elevated ducts trap EM waves only from sources at altitude, making a radar's detection of targets within the duct more likely than targets outside of it.

Solar heating during the day will alter the height of an elevated duct resulting in a vertical meandering. These types of ducts occur more than 50% the time and have an average height of 3 km to a maximum of approximately 6 km.

3. Evaporation Ducts

An evaporation duct is caused by rapid vertical decrease in humidity from the air/sea interface. As can be seen in Figure 3.7 the modified refractivity M , decreases rapidly with height only to reach a minimum near the surface and begin to increase with height. The height where M reaches a minimum is the evaporation duct height. These ducts are

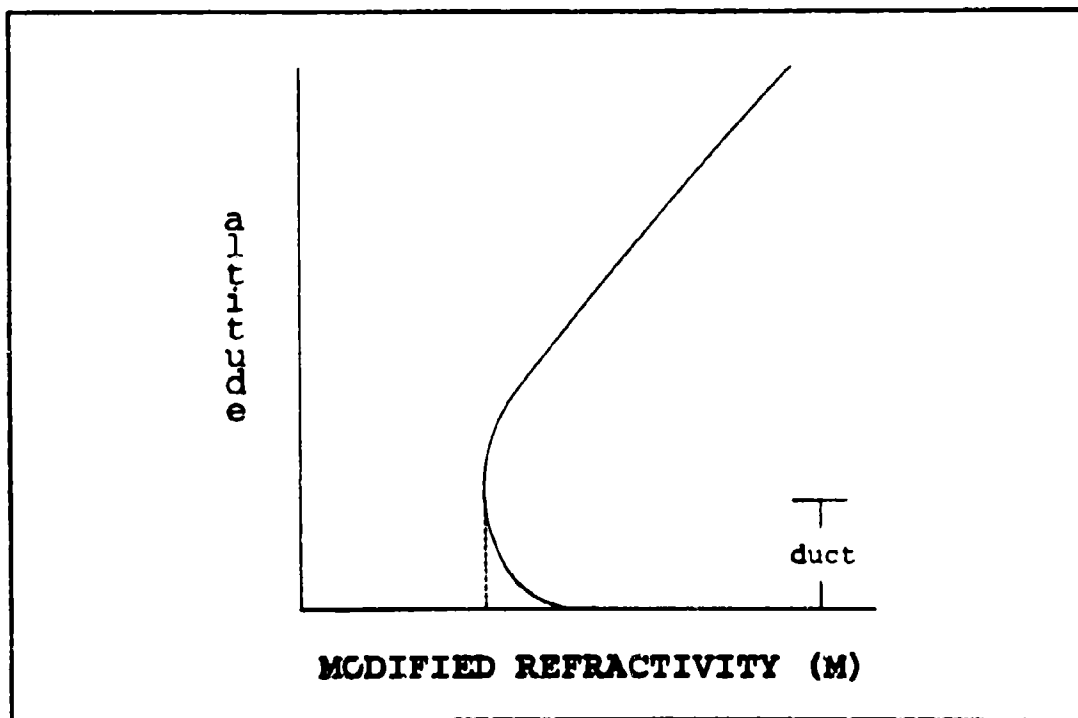


Figure 3.7 Evaporation Duct.

normally under 30 meters in height and have a 13 meter worldwide average. EM systems with frequencies greater than 3 GHz are affected by the evaporation duct. These ducts are usually present all the time.

Considering the average duct height is 14 meters, it would seem possible to measure the evaporation duct directly. The nonhomogeneity of the lower atmosphere makes this almost impossible. Any single atmospheric profile would not represent the average evaporation ducting conditions.

E. SEA CLUTTER

The sea surface usually consists of an irregular distribution of shapes and sizes of waves. Wind speed and direction, swell height and direction, and biologics can affect radar returns from the surface of the sea. The radar return from the sea surface is dependent on frequency, polarization, and grazing angle of the radar system utilized. (Skolnik, 1980, p. 474)

Ducting such as surface-based or evaporation duct will enhance sea clutter returns. Beach (Beach, 1980, p. 83) explains why it can be more difficult to discriminate small targets, such as submarine periscopes from background noise. Multiple false targets will make detection of low radar cross section targets extremely difficult.

Surface-based ducts usually yield range periods of high sea clutter independent of azimuth angles. However,

evaporation ducts result in enhanced sea clutter returns with range. Sea clutter of either type results in masking of areas from radar detection of actual targets.

(Dockery, 1991, p. 3-46)

There are several models for calculating average values of sea clutter returns. The EREPS model used in this analysis contains a Naval Ocean Systems Center modified model of the original developed by the Georgia Institute of Technology (GIT) and is discussed in Appendix B.

F. IN SITU COLLECTION

1. Shipboard Influences

The refractive properties of the surface evaporation duct are dependent upon the air temperature and moisture profiles immediately above the ocean surface. Models such as the Integrated Refractive Effects Prediction System (IREPS), described in Appendix B, require the accurate measurement of wind speed, sea surface temperature, air temperature, and relative humidity.

Temperature measurement has always been a problem. Air temperature measurement is highly dependent on location since thermal influence of the ship contributing to errors. Water temperature is typically measured at the seawater intake for engine cooling. Readings are usually obtained from gauges in the power plant spaces by engine-room personnel. The intakes are located well below the surface and lend themselves to

errors induced by thermal contamination, calibration, and poor reporting standards.

Even more important than absolute accuracy in air and sea temperature measurement is relative accuracy. Differences between air and sea temperature are generally small, and under certain conditions large errors result in the calculation of duct height. The relative accuracy of the air-sea temperature difference is most important for these cases since this difference has the greatest effect on the calculated duct height. (Cook, 1991, p. 731-746)

IV. EREPS SEA CLUTTER PREDICTION - MID-ATLANTIC COAST SCENARIO

A. INTRODUCTION

EM ducting, caused by surface-based or evaporation ducts will enhance sea clutter returns. This usually makes it more difficult to discriminate small targets, such as submarine periscopes from background noise or false targets. Multiple false targets will make detection of low radar cross section targets extremely difficult.

This chapter presents a comparison of sea clutter prediction using the EREPS (PROPR) program and actual high-power surveillance scans obtained from Space and Ranging Radar (SPANDAR) research radar. SPANDAR is operated by the National Aeronautics and Space Administration (NASA) Wallops Flight Facility (WFF). SPANDAR is a high power S-band research radar used mostly in atmospheric experiments. SPANDAR's sensitivity enables it to image air turbulence and sea clutter. SPANDAR data was collected via clutter maps providing real-time indication of propagation conditions.

In August 1990 Johns Hopkins University Applied Physics Laboratory (JHU/APL) conducted a field experiment in the SPANDAR field of view. The experiment was Demonstration Test (DT-1, Phase 3) designed to test the operation of the first-generation Cooperative Engagement Capability (CEC) system. CEC

was developed under the Battle Group Antiair Warfare Coordination (BGWAAWC) program in a realistic projected tactical environment.

JHU/APL obtained environmental data was interpreted with EREPS (PROPR) radar signal-to-noise ratio program which provides propagation loss in dB versus range and sea clutter level displayed by superimposing a plot of the ratio of clutter-to-noise power. It can be used in determining the maximum detection ranges and sea clutter effects.

Values for the environmental parameters entered into the EREPS (PROPR) program were obtained from an instrumented 50-ft boat, C^UESSIE, owned and operated by JHU/APL. The boat collected sea surface and air temperature, humidity and wind speeds at various heights. Ducting conditions and evaporation duct height was determined using a version of the Paulus model.

Two cases will be presented. Case 1 will deal with a weak surface-based duct and strong evaporation duct. Case 2 will look at a strong surface-based duct. EREPS signal-to-noise ratio model within the PROPR program will be used to derive sea clutter predictions based on environmental data taken on scene and SPANDAR system parameters employed.

**B. CASE 1 - WEAK SURFACE-BASED DUCT AND STRONG EVAPORATION
DUCT - 1430 15 AUGUST 1990**

1. Environment

The offshore environmental conditions for Case 1, 15 August 1990 at 1430, consist of a weak surface based duct (Figure 4.1) and a strong evaporation duct height of 25 meters (Figure 4.2). Figure 4.2 illustrates that the evaporation duct height determined using a prediction model is more of measure of strength of the duct. It certainly is not necessarily a hard upper boundary height of the duct for trapping EM waves and yielding extended ranges. The relatively vertical portion of the curve above 25 meters shows that the upper boundary of our duct is very weak in comparison to the lower, sea surface. Therefore antenna placement below or above the predicted upper limit of the evaporation duct is not as critical to yielding extended ranges as is simply operating in the presence of a strong evaporation duct.

The Figure 4.1 profile suggests boundary layer conditions bordering between subrefraction and trapping. Hence, in this situation the 25 meter evaporation duct was the major influence on propagation.

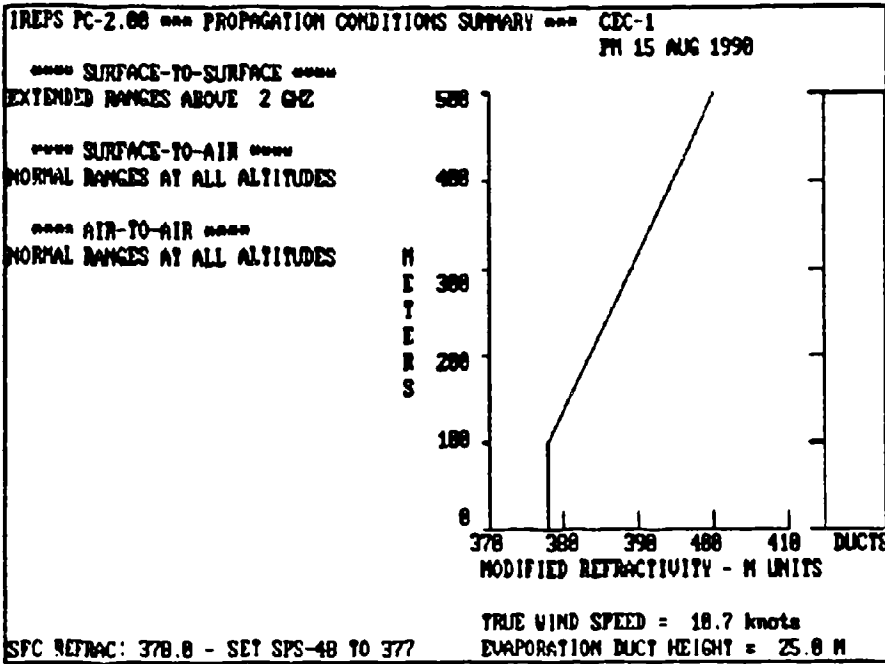


Figure 4.1 IREPS M-profile for PM 15 August 1990 (Case 1).

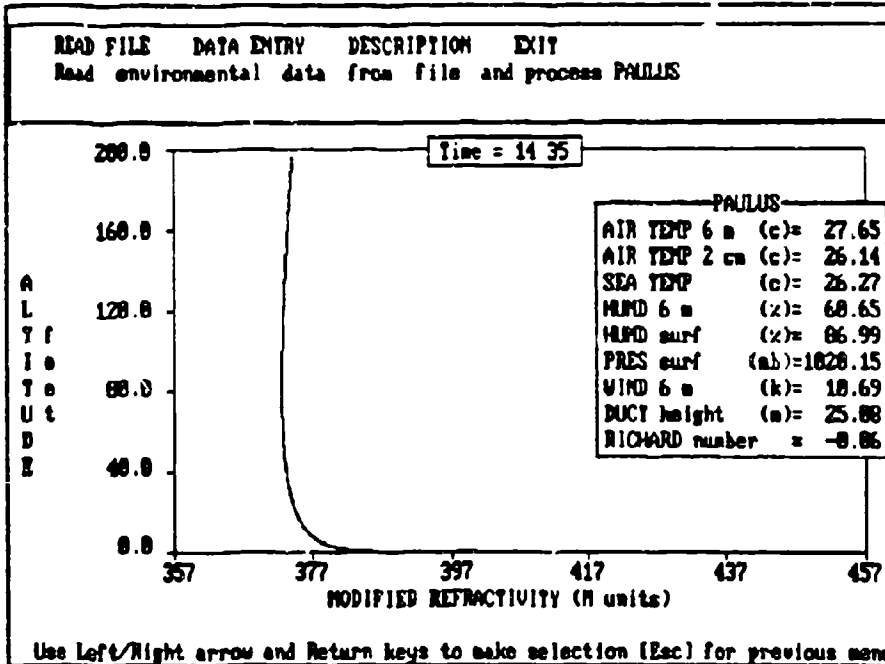


Figure 4.2 Evaporation duct M-profile using Paulus Model (Case 1).

2. Radar Performance Analysis

a. Radar Observations

The SPANDAR PPI scan (display) shown in Figure 4.3 illustrates the influences of a strong evaporation duct with a possible weak surface-based duct. The display shows how a strong evaporation duct extends the sea clutter horizon with

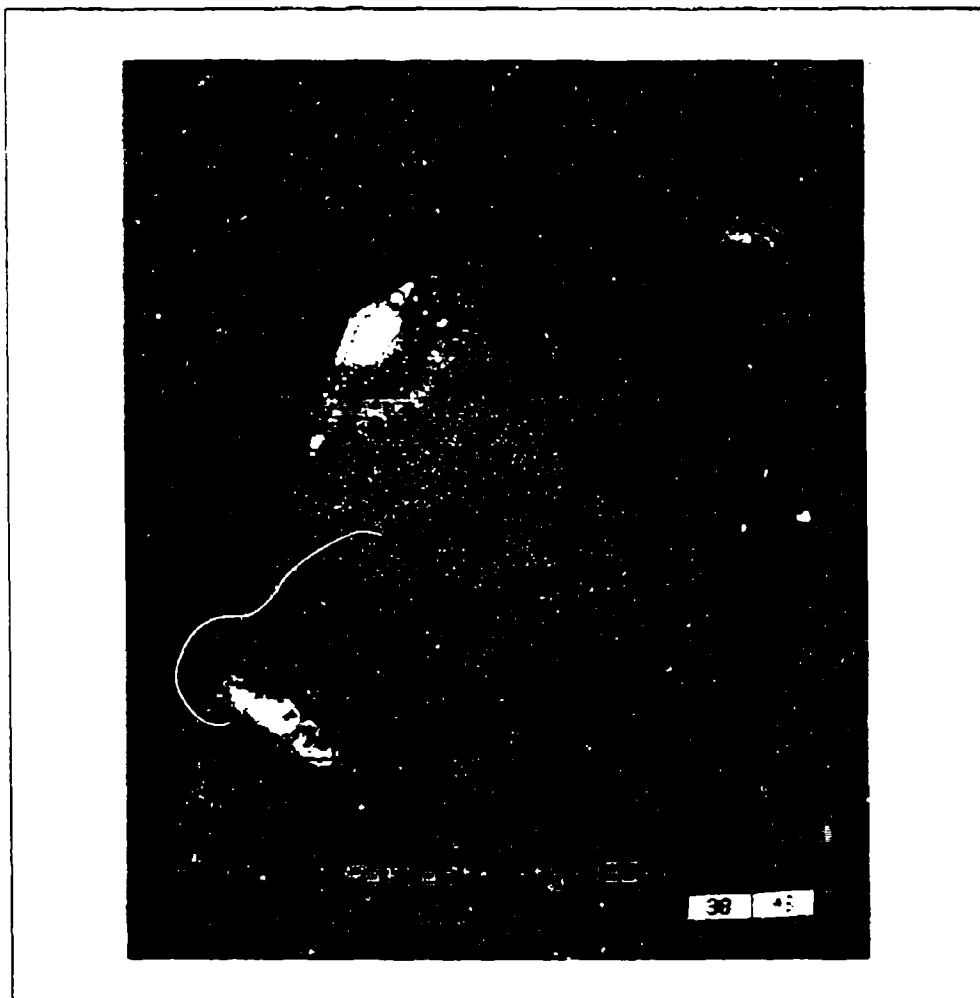


Figure 4.3 SPANDAR PPI Scan for 1430 15 August 1990 (Case 1).

sporadic points of higher reflectivity. This can be attributed to increased clutter to signal ratio due to enhancement of sea clutter by the presence of the strong evaporation duct.

b. EREPS Prediction

The EREPS loss prediction including sea clutter is shown in Figure 4.4. Depicted on this graph is radar signal-to-noise level plotted against range. Sea clutter level, (short-dashed line) is shown by a plot of the ratio of clutter-to-noise power versus range. Sea clutter model used in EREPS is the Georgia Institute of Technology (GIT) code described in Appendix B. Entering arguments were the basic

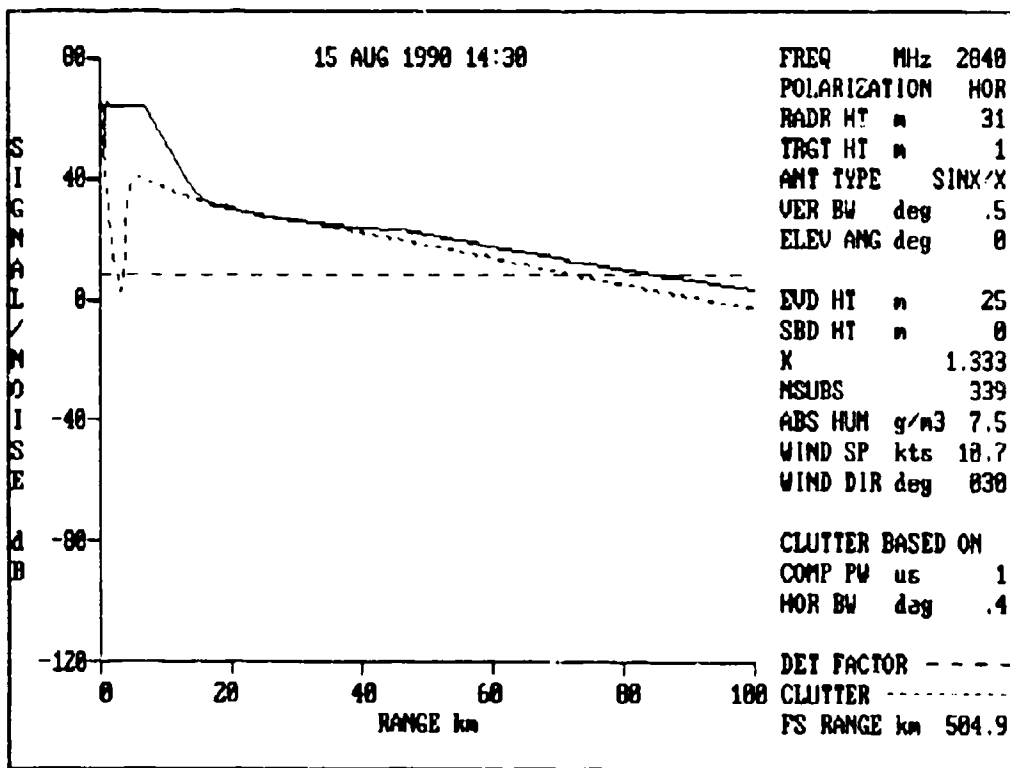


Figure 4.4 EREPS loss prediction for 15 AUG 90 (Case 1).

operating parameters of SPANDAR. The relatively close overlap of the sea clutter and signal-to-noise ratio curves observed in Figure 4.4 explains the random or sporadic clutter points on the SPANDAR PPI scan. This interpretation is based on a margin for error or inhomogeneity of the atmosphere not accounted for in the model.

The comparison of the EREPS evidence of sea clutter and actual radar performance indicates that EREPS can be a useful tool to the tactician in selecting and utilizing a sensor.

A tactical planner would take this to indicate sea clutter will affect his system performance but not white out his scope. Knowledge of sea clutter can influence sensor selection and their settings, to best exploit the environmental conditions encountered.

C. CASE 2 - STRONG SURFACE-BASED DUCT - 1930 12 AUGUST 1990

1. Environment

Atmospheric conditions for Case 2, on 12 August 1990 at 1930, included a strong surface-based duct and a weak evaporation duct. As shown in Figure 4.5, the surface-based duct is formed by the trapping layer; extending from below 200 to above 400 meters. The evaporation duct M-profile depicted in Figure 4.6 is near 15 meters and is approximately 12 meters smaller than for Case 1. Therefore, the significant difference between Case 1 and Case 2 is the presence of a strong surface-based duct of approximately 450 feet (150 meters).

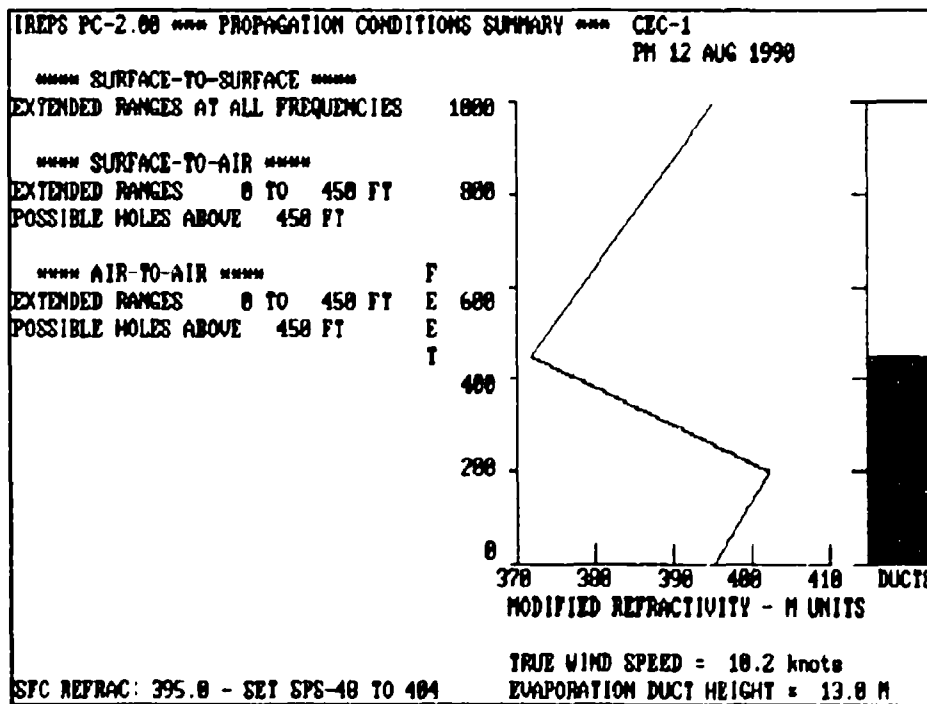


Figure 4.5 IREPS M-profile for PM 12 August 1990 (Case 2).

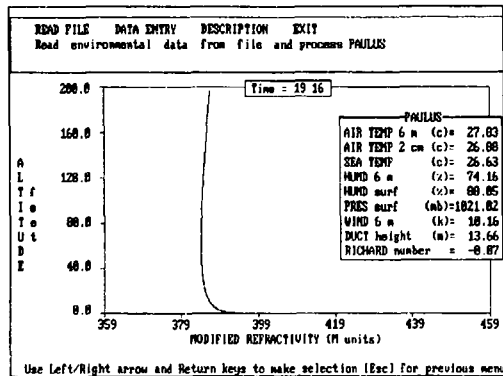


Figure 4.6 Evaporation duct M-profile using Paulus Model (Case 2).

2. Radar Performance Analysis

a. Radar Observations

Figure 4.7 reveals an extended clutter horizon as a result of the evaporation duct and a clutter ring concentrated in the 30 to 60 nm range. The clutter rings are associated with radar energy being reflected off the inversion layer of the strong surface-based duct. Inside the clutter ring range of 30 nm lies the area of increased sea clutter.

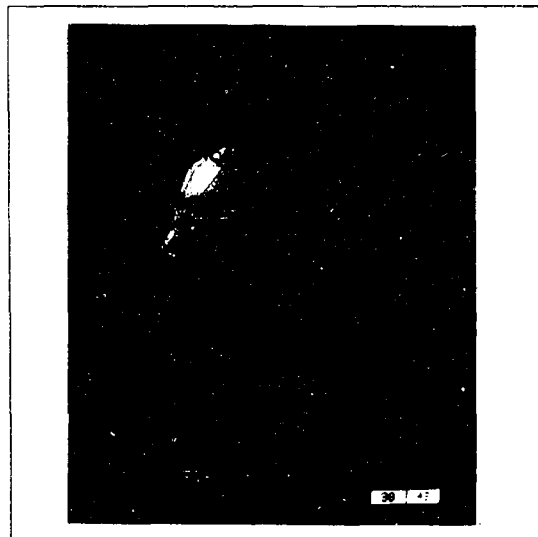


Figure 4.7 SPANDAP PPI Scan 1936 12 August 1990 (Case 1).

b. EREPS Prediction

The difference between the EREPS clutter prediction represented in Case 2 (Figure 4.8) and Case 1 (Figure 4.4) is due to Case 2 having a 12 meter shorter evaporation duct and a strong 150 meter surface-based duct. Figure 4.8 reveals the sea clutter curve (dotted-line) surpassing the radar signal-to-noise curve (solid-line) from approximately 25 kilometers to 61 kilometers illustrating a probable region of enhanced sea clutter returns affecting the sensor. The signal-to-noise ratio curve has a negative slope starting at about 7 kilometers reaching a low of -18 dB at

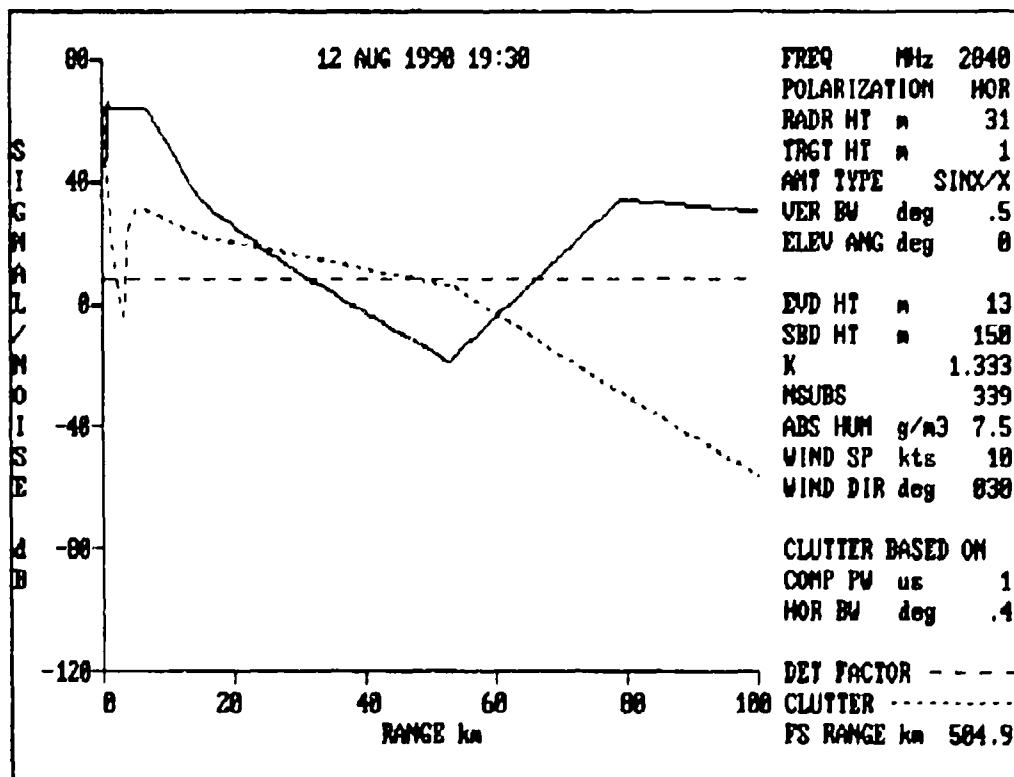


Figure 4.8 EREPS loss prediction for PM 12 August 1990 (Case 2).

approximately 52 kilometers then a positive slope to 79 kilometers. The curve below the detection factor line (horizontal dotted-line) indicates an area of reduced or no sensor detection.

These conditions would indicate to the tactician that an alternative sensor and/or different operating parameters should be used.

D. SUMMARY

These results have shown the influence of atmospheric refraction of sea clutter which could degrade surveillance radar performance. They also show how carefully and comprehensively collected CEC-1 data resulted in the EREPS predictions closely matching actual observations. The presence of the strong surface-based duct had a significant impact on the sea clutter and radar detection range prediction. As a result it is clear that rawinsonde data is vital to the accurate assessment of the environment in which a sensor is operated. With this knowledge, searches can be more efficiently carried out and the user can better understand exactly how well an area was covered after a search was conducted.

V. COMPARISON OF EFFECT ON DIFFERENT GENERIC SURVEILLANCE RADAR SENSORS - GULF OF OMAN

A. INTRODUCTION

Field data for this part of the thesis were obtained during SHAREM 102 conducted in the Gulf of Oman (Figure 5.1) during January 1993. SHAREM 102 consisted of structured and freeplay events in the Gulf of Oman in three different areas along the coast of Iran.

The meteorology of the Gulf of Oman is characterized by seasonal monsoon winds. The term "monsoon" denotes a trend for the winds to blow persistently from the same direction for a season, and just as persistently from a different direction for another season. In the winter (December through March) period of this study, the winds blow from the northeast. Elevated ducts occur more frequently in the winter.

The polar air mass from the northeast, modified somewhat by contiguous mountain ranges, is met by the tropical marine air over the Arabian Sea. Wind speed average around 10 knots over the northern part of the Arabian Sea, increasing to around 20 knots to the south.

The environmental conditions encountered during SHAREM were persistent. For this discussion only one example is examined, which is a good representation of conditions encountered during the the entire experiment. Winds were

generally light, from calm to 7 knots. These light conditions were caused by a stationary continental high pressure regime in the north of Iran. The passage of a low pressure system over the Arabian Gulf on 10 January was accompanied by higher winds of approximately 10 knots. The sea state was low with no swell. However, waves during stronger winds never exceeded three feet. Visibility was normally unlimited, with slight haze accompanying winds from the north.

An overview of refractive conditions is that elevated ducts were present as evidenced in atmospheric profiles shown later. Atmospheric ducting appeared to have no effect on

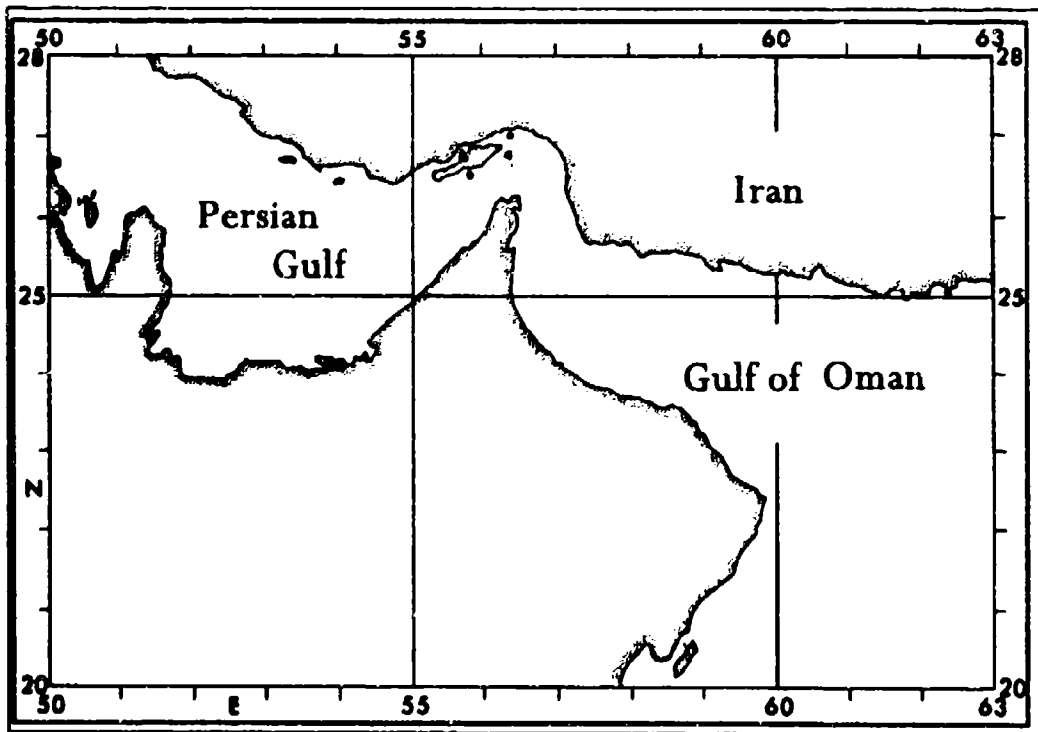


Figure 5.1 Arabian Gulf and Gulf of Oman Map (Case 3).

periscope detections. It is believed this arose even with variable refractive conditions because the ship-submarine separation never exceeded the visible horizon. This is not to conclude that ducting conditions did not yield detection range differences, but that range differences between sensor and target never allowed verification of extended ranges when strong evaporation duct was present.

Rawinsondes indicated the presence of a strong evaporation duct on several occasions yielding extended detection ranges for frequencies greater than 1 GHz to 4 GHz. This is tactically significant for the ASW decision maker. Since it permits a much larger area to be searched with available sensors. In most cases up to five times the area than without ducting.

B. GENERIC SURVEILLANCE RADAR SENSOR PARAMETERS

We examine the influences of meteorological conditions in the Gulf of Oman during SHAREM 102 on five generic radar systems. Collected data and parameters are used as input for IREPS, EREPS and RPO programs (Appendix B). IREPS will be used primarily to show refractive conditions. EREPS, which includes IREPS propagation codes, will be used to identify propagation loss versus range values and sea clutter prediction. RPO will be used to display propagation loss downrange performance for horizontally inhomogeneous environments and illustrate how the effects of anomalous propagation can lead to coverage holes and enhanced clutter.

Radar Sensor	Operating Freq (GHz)	Antenna Height (ft/m)	Polarization
I	0.4	100/30.5	Horizontal
II	1.3	55/16.8	Horizontal
III	1.3	90/27.4	Vertical
IV	9.5	70/21.3	Horizontal
V	9.5	140/42.7	Horizontal

Table 5.1 Generic Radar Sensor Parameters for Case 3.

C. CASE 3 - 0927/0939L 08 JANUARY 1993 RAWINSONDES

Case 3 consists of taking the meteorological data from two rawinsonde launches, separated by 29 kilometers and 12 minutes in time and applying it to the five generic radar systems. The time difference between rawinsonde launches is considered to be insignificant.

1. Environment

The relevant meteorological conditions for Case 3, on 8 January 1993 are described on the basis of a 0927L launch at 24.92N 060.72E and a 0939L launch at 24.83N 060.45E from two different ships. Figures 5.2 and 5.3 show elevated ducts for both launches. The elevated ducts are well above the height of the antenna of all five generic sensors.

The only difference between the two profiles is thickness of the elevated duct and the 0927L launch has a 5 meter less thick evaporation duct. This is not a significant difference when comparing frequency dependence or M-profile curves of the duct.

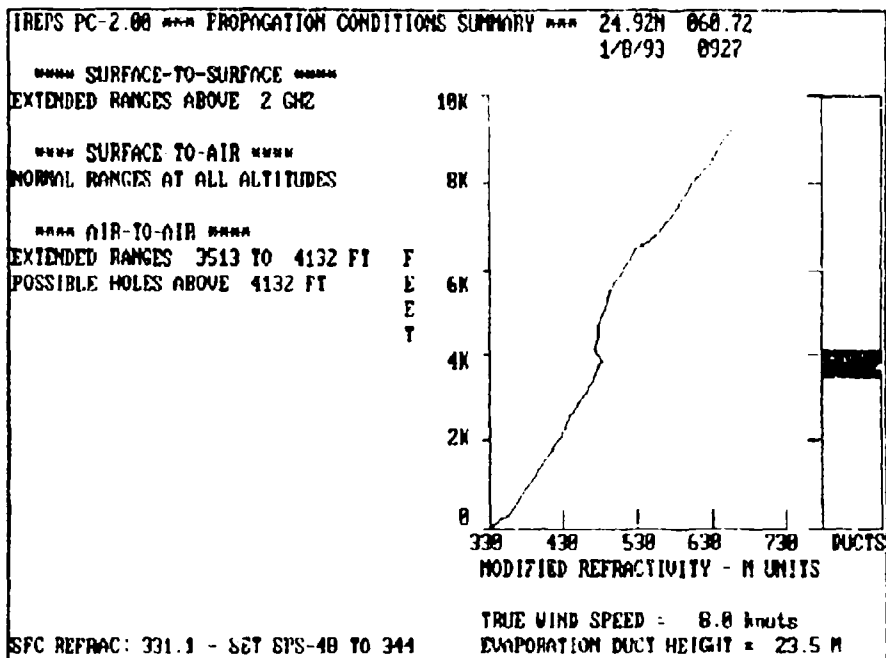


Figure 5.2 IREPS M-profile for 0927 08 JAN 93
(Case 3).

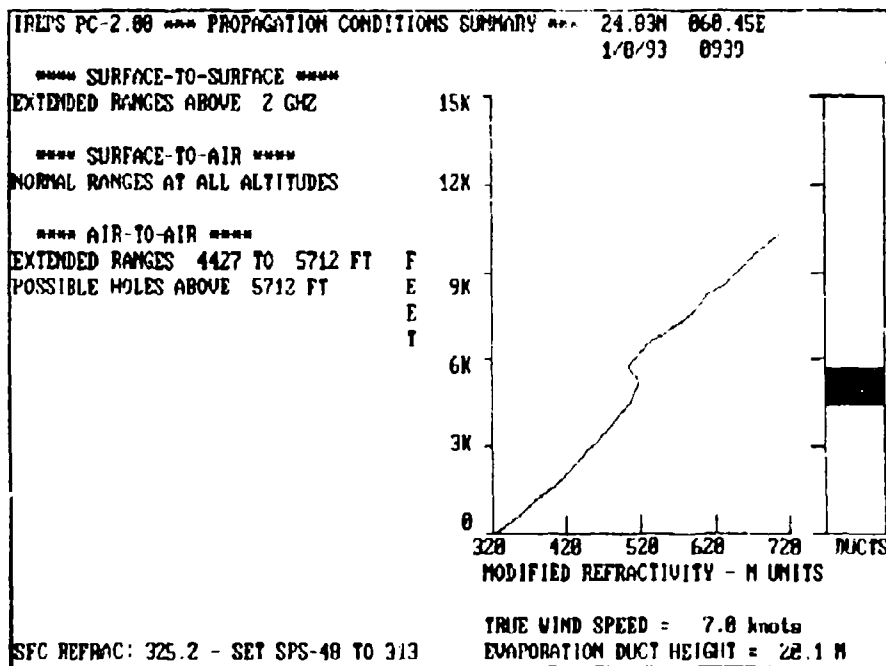


Figure 5.3 IREPS M-profile for 0939 08 JAN 93
(Case 3).

2. Generic Surveillance Radar Sensor Performance Analysis

a. Generic Radar - Sensor 1 Analysis

Sensor 1 is 400 MHz horizontally polarized radar with an antenna height of 30 meters. Sensor 1 EREPS PROPR signal-to-noise ratio prediction results are shown in Figure 5.4 for SHAREM 0939L January 1993 rawinsonde data and the standard atmosphere. The radar free-space range is 100.2 km. RPO plots of encountered and standard atmosphere conditions are shown in Figures 5.5 and 5.6 respectively.

EREPS predicts only slightly enhanced ranges for the target curve with the presence of the 23.5 meter evaporation duct, while sea clutter receives a 10 dB increase at the 40 km range over the standard atmosphere curve. RPO tends to back up this prediction as Figure 5.6 shows only a slight increase in loss with the appearance of the 140 dB loss region at 25 km through to 30 km.

Sensor 1's low operating frequency of 400 MHz can be held accountable for the evaporation duct having little effect on detection or sea clutter. The assessment is based on enhancements over standard atmosphere conditions. The evaporation duct is thinner than surface-based ducts, so its influence is very frequency dependent. Frequencies below 3 GHz are usually only minimally affected by the evaporation duct.

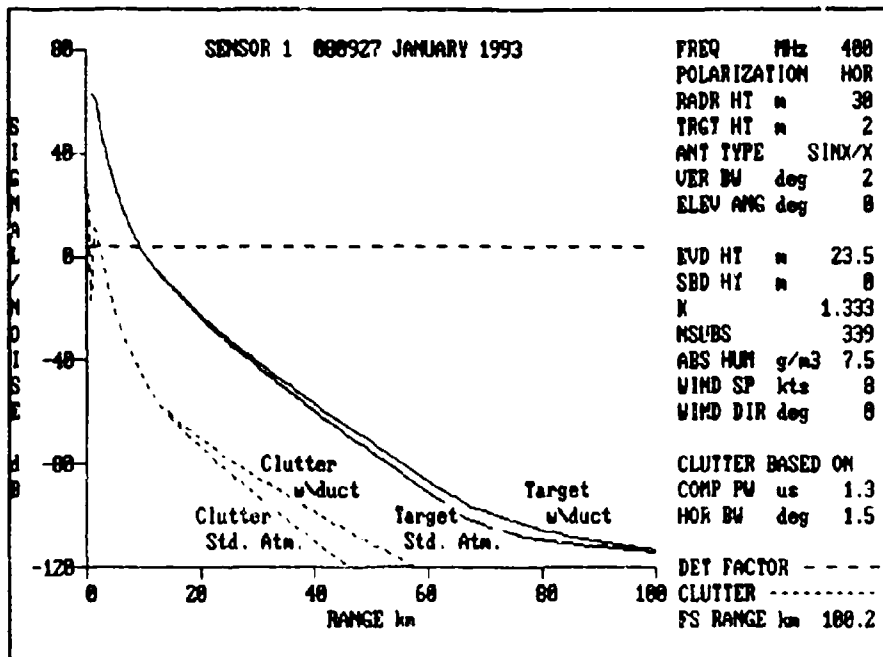


Figure 5.4 EREPS Sea Clutter prediction for Sensor 1 (Case 3).

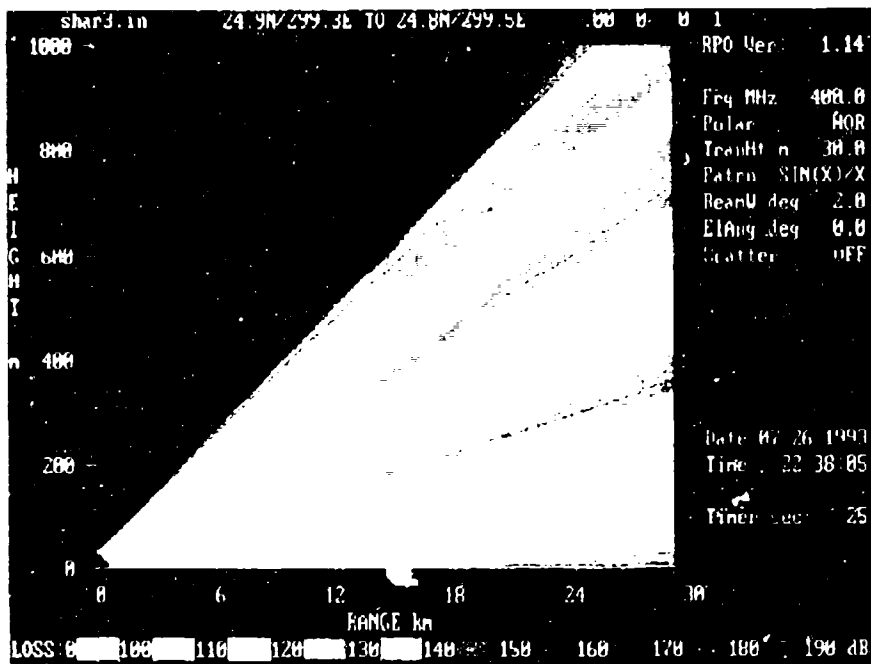


Figure 5.5 RPO Plot of Sensor 1 0927L 08 JAN 93

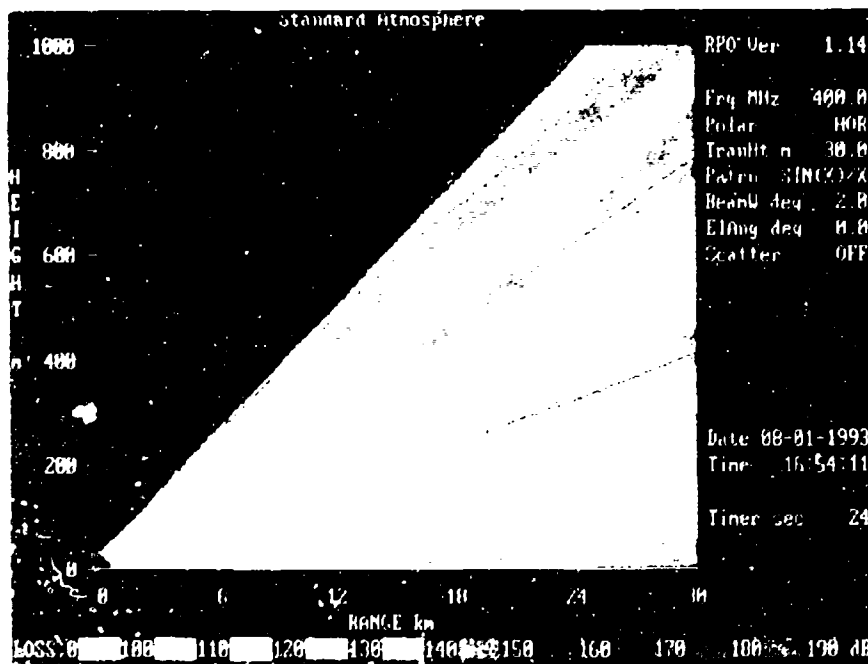


Figure 5.6 RPO Plot of Sensor 1 in Standard Atmosphere Conditions Case 1

b. Generic Radar - Sensor 2 Analysis

Sensor 2 is a 1.3 GHz horizontally polarized radar at a height of 17 meters. Sensor 2's EREPS PROPR signal-to-noise ratio prediction results are shown in Figure 5.7 for SHAREM 0927L 08 January 1993 rawinsonde data and standard atmosphere. The radar free-space range is 55.6 km. RPO plots for SHAREM and standard atmosphere conditions are shown in Figures 5.8 and 5.9 respectively.

EREPS predicts enhanced ranges with approximately a 35 dB increase in target detection with the presence of the 23.5 meter duct at the 56 km range. The target curve is close to 45 db stronger than the sea clutter curve indicating that clutter would not interfere with target detection. Sea clutter is enhanced but not to the point of overcoming target detection. RPO SHAREM plot (Figures 5.8) indicates a 130 dB loss at zero elevation at 28 km while the standard atmosphere case (Figure 5.9) is showing a 170 dB loss at the same height and distance. This is the same trend, but a slightly higher loss than the EREPS prediction.

Sensor 2 is not strongly affected by the presence of the evaporation duct due to its relatively low operating frequency. This outcome is similar to that of Sensor 1.

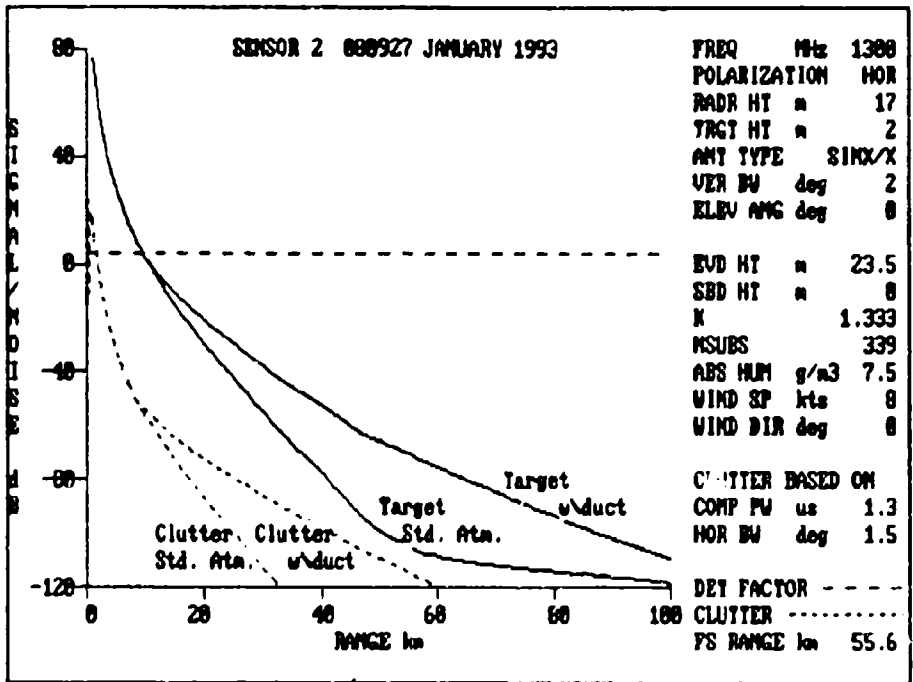


Figure 5.7 EREPS Sea Clutter prediction for Sensor 2 (Case 3).

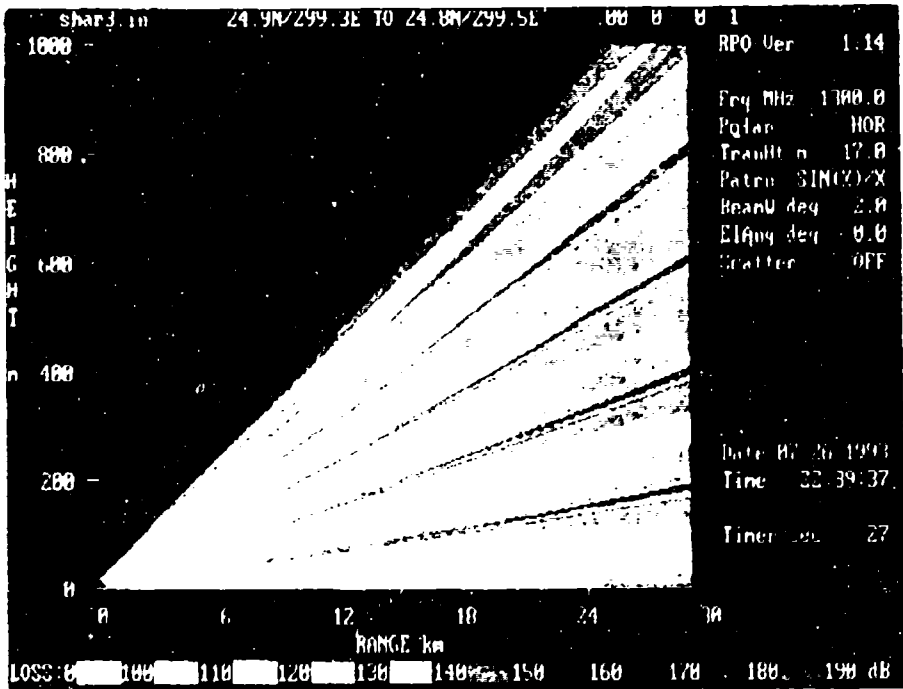


Figure 5.8 RF Plot of Sensor 2 0927L 88 JAN 93 6
Case 1

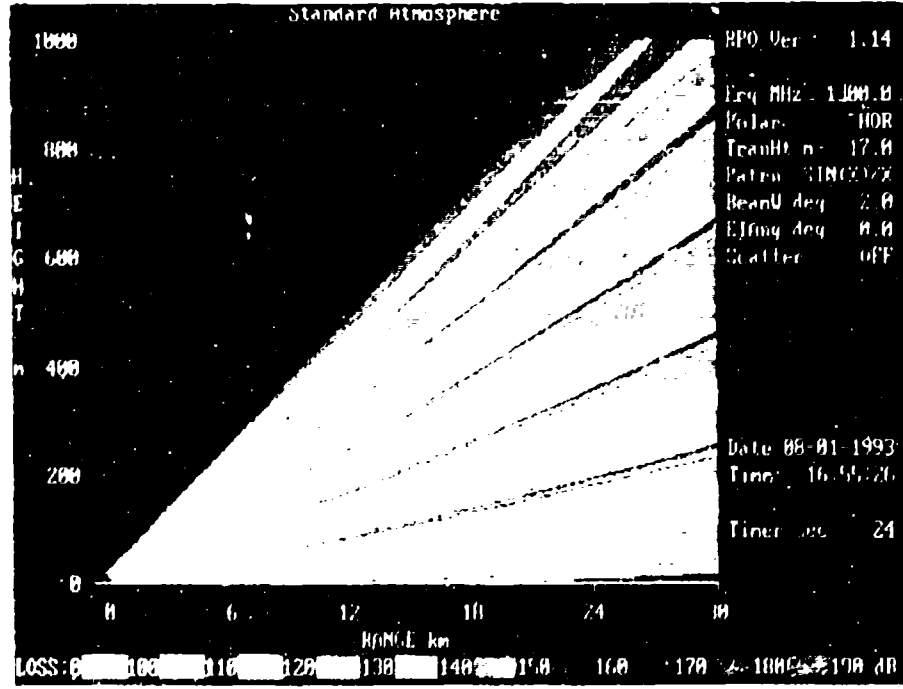


Figure 5.9 RF Plot of Sensor 2 in Standard
Atmosphere 0927L 88 JAN 93 6
Case 1

c. Generic Radar - Sensor 3 Analysis

Sensor 3 is a 1.3 GHz vertically polarized radar with an antenna height of 27 meters. Its EREPS PROPR signal-to-noise ratio prediction is shown in Figure 5.10 for SHAREM 0927L 08 January 1993 rawinsonde data and standard atmosphere. The radar free-space range is 55.6 km. RPO plots of SHAREM and standard atmosphere conditions are shown in Figures 5.11 and 5.12 respectively.

EREPS predicts enhanced target detection and sea clutter. Target detection has a 40 dB increase at approximately 60 km, while sea clutter enjoys a 30 dB enhancement at 38 km and is at -120 dB at 65 km. As in Sensor 2's prediction sea clutter is enhanced but not to the point of overwhelming the target detection curve.

RPO SHAREM plot (Figure 5.11) indicates a 130 dB loss at at zero elevation at 25 km while the standard atmosphere case is showing a 140 db loss at the same altitude and range. Once again RPO appears to mirror EREPS prediction.

Sensor 3, as with Sensors 1 and 2 is not strongly affected by the presence of the evaporation duct due to its relatively low operating frequency. It is noted that EREPS plots for Sensors 2 and 3 are almost identical. Sensor 3 antenna height is 10 meters higher and is vertically polarized vice horizontally like Sensor 2. Of some signifigance is that the RPO plots for the SHAREM atmosphere conditions are

virtually the same at lower elevations, but the standard atmosphere plots indicate Sensor 2 has a greater loss with a 150 dB loss appearing at the 25 km range at zero elevation.

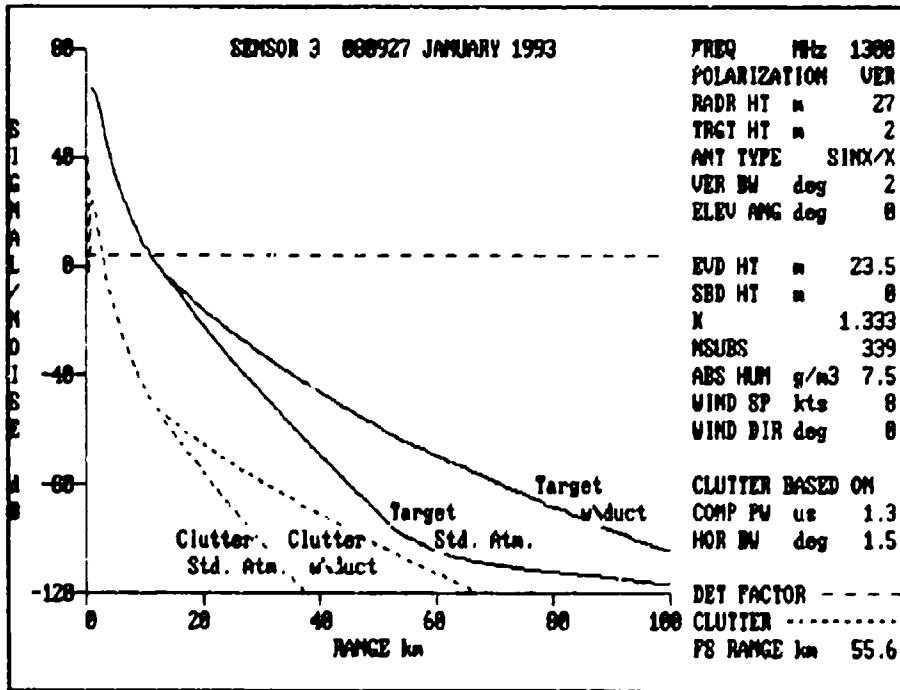


Figure 5.10 EREPS Sea Clutter prediction for Sensor 3 (Case 3).

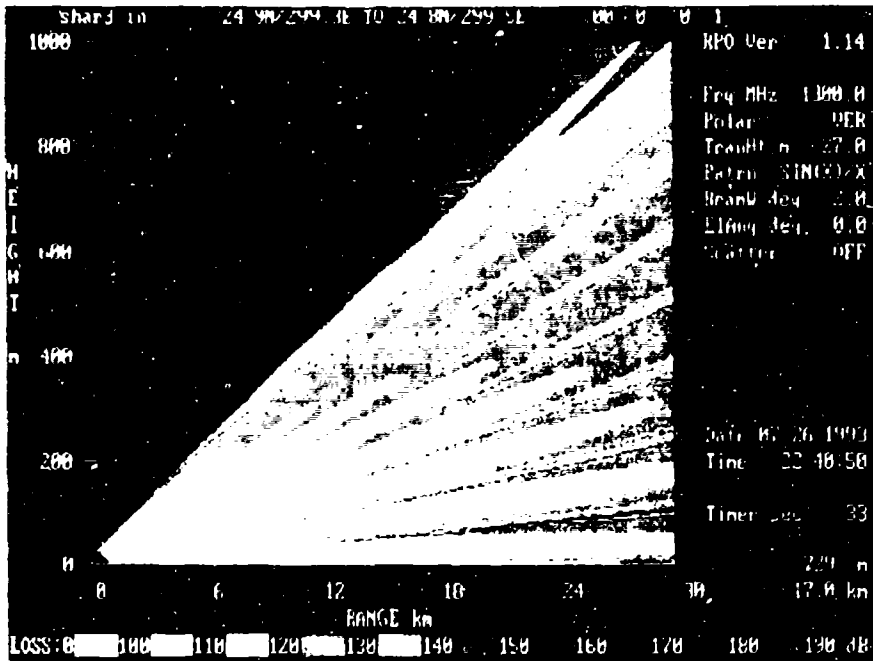


Figure 5.11 RPO Plot of Sensor 3 0927L 08 JAN 93
Case 3

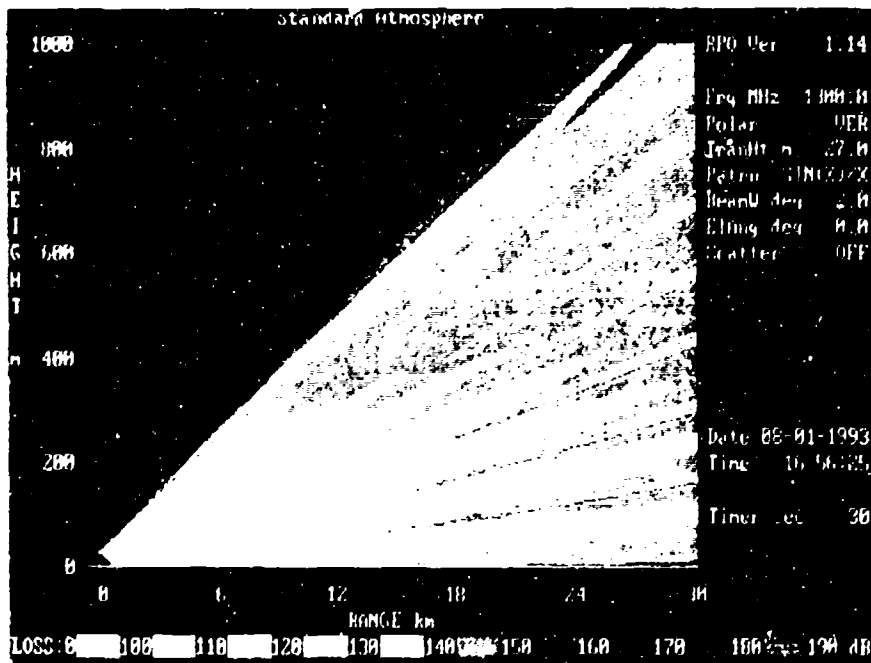


Figure 5.12 RPO Plot of Sensor 2 in Standard
Atmosphere Conditions Case 3

d. Generic Radar - Sensor 4 Analysis

Sensor 4 is 9.5 GHz horizontally polarized radar with an antenna height of 27 meters. EREPS PROPR signal-to-noise ratio prediction are shown in Figure 5.13 for SHAREM 0927L 08 January 1993 rawinsonde data and standard atmosphere. The radar free-space range is 20.6 km. RPO plots of SHAREM and standard atmosphere conditions are shown in Figures 5.14 and 5.15 respectively.

EREPS depicts a radical difference in predictions between an atmosphere without and with the presence of the 23.5 meter evaporation duct. As would be expected in standard atmosphere conditions the target curve is above the sea clutter curve. But, with evaporation duct present, at 26 km the target curve receives a 20 dB enhancement while the sea clutter increases by 105 dB. Sea clutter is enhanced to the point that its curve dominates the target curve by a minimum of 10 dB from 21 km out to the end of the plot. This would signify sea clutter to be a significant degradation to radar performance beyond the 21 km range.

The RPO SHAREM plot (Figure 5.14) indicates a 130 dB loss at zero altitude from 17 to 27 km while the standard atmosphere case (Figure 5.15) shows 140 dB loss from 17 to 22 km followed by 150 dB loss from 22 to 27 km which is followed by a 160 dB loss from 27 to 30 km. RPO indicates extended

ranges but does not differentiate the enhancement between target signal or sea clutter.

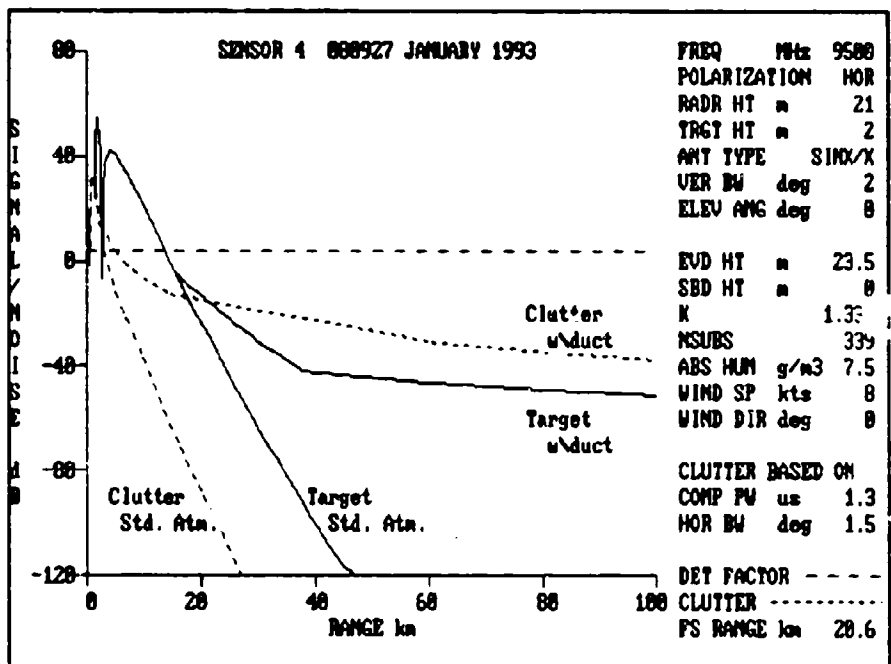


Figure 5.13 EREPS Sea Clutter prediction for Sensor 4 (Case 3).

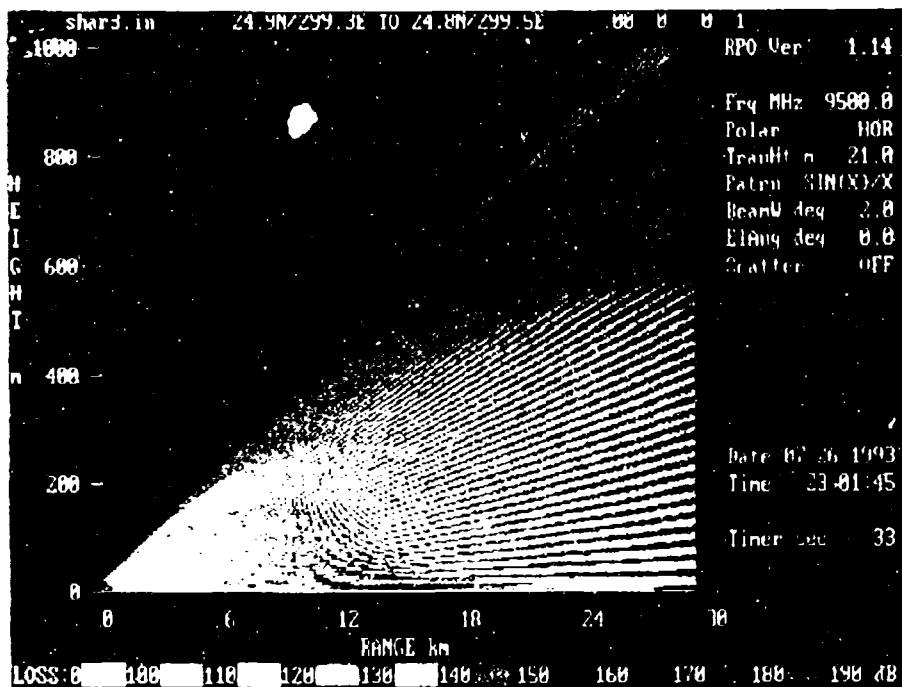


Figure 5.14 RPO Plot of Sensor 4 0927L 08 JAN 93
Looking Seaward Case 4.

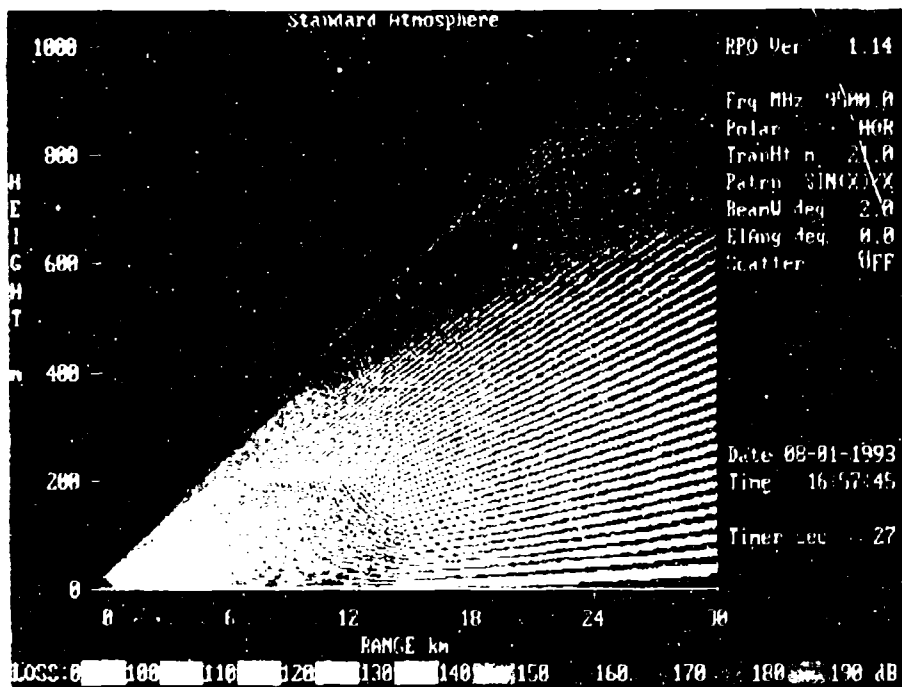


Figure 5.15 RPO Plot of Sensor 4 in Standard
Atmosphere Conditions Case 3

Previous applications of the RPO model has been with the generic radar sensors using the point closest to shore and looking towards the more seaward rawinsonde profile location. An examination was conducted where the profiles were reversed. That is the sensors were essentially looking from the seaward point towards shore.

The outcome of these examinations were that Sensors 1 through 3 encountered little to no affect by this reversal, but Sensors 4 and 5 saw a significant difference in RPO's propagation profile.

With the radar looking towards shore (Figure 5.16) as compared to the sensor looking seaward (Figure 5.14) an interesting conclusion can be drawn. It appears that under these conditions radar performance is enhanced when looking towards shore vice looking seaward. The significant difference is the height of the evaporation duct at the two points. The profile farthest from shore (Figure 5.3) depicts a weaker evaporation duct while the profile closest to shore (Figure 5.2) shows a stronger duct. From this one can readily draw the conclusion that a radar sensors detection range is enhanced when looking from an area with a weak evaporation duct profile in the direction the duct strengthens.

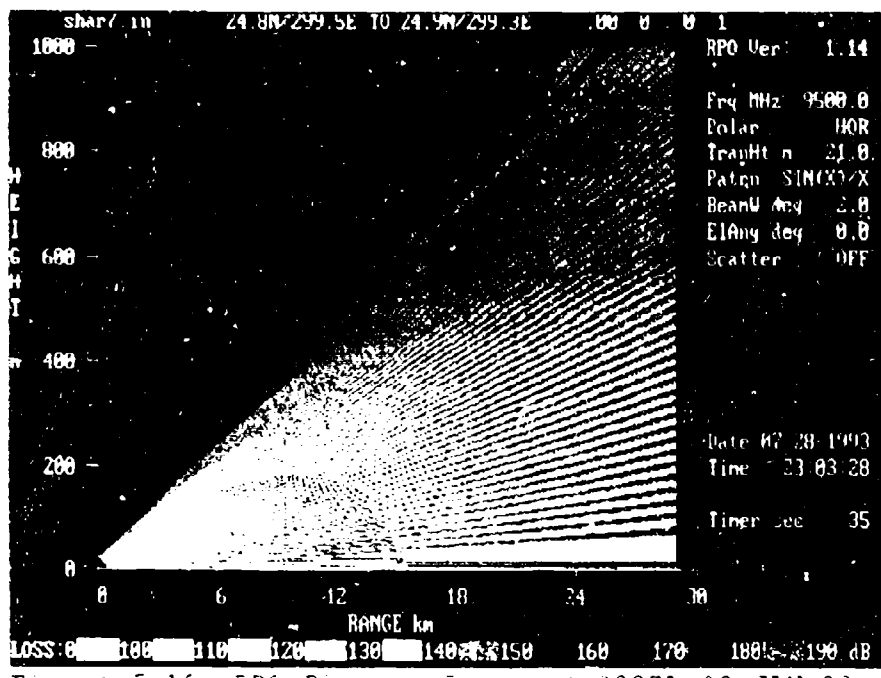


Figure 5.16 RPO Plot of Sensor 4 19272 28 JAN 93
 Looking Towards Shore - Case 3

e. Generic Radar - Sensor 5 Analysis

Sensor 5 is 9.5 GHz horizontally polarized radar with an antenna height of 43 meters. EREPS PROPR signal-to-noise ratio prediction results are shown in Figure 5.17 for SHAREM 0927L 08 January 1993 rawinsonde data and standard atmosphere conditions. The radar free-space range is 20.6 km. RPO plots of SHAREM and standard atmosphere conditions are shown in Figures 5.18 and 5.19 respectively.

As in Sensor 4's analysis, EREPS depicts a drastic difference in predictions between an atmosphere without and one with the 23.5 meter evaporation duct present. As before in standard atmosphere conditions the target curve is above the sea clutter curve. But, with evaporation duct present, at 32 km the target curve receives a 27 dB enhancement while the sea clutter increases by 100 dB. Sea clutter is enhanced to the point that its curve dominates the target curve by a minimum of 10 dB from 30 km out to the end of the plot. This would signify sea clutter to be a significant degradation to radar performance beyond the 30 km range, 9 km greater than Sensor 4. Sensor 5 antenna is just above the 23.5 evaporation duct while Sensor 4 antenna is just below it. Therefore, EREPS predicts longer ranges for an antenna above the evaporation duct rather than below the duct.

The RPO SHAREM plot (Figure 5.18) indicates a 140 dB loss at zero altitude from 21 to 27 km and a 150 dB loss

from 27 to 29 km, while the standard atmosphere case (Figure 5.19) shows 140 dB loss from 23 to 29 km followed by 150 dB loss from 29 to 30 km. RPO indicates reduced ranges which contradicts the EREPS prediction.

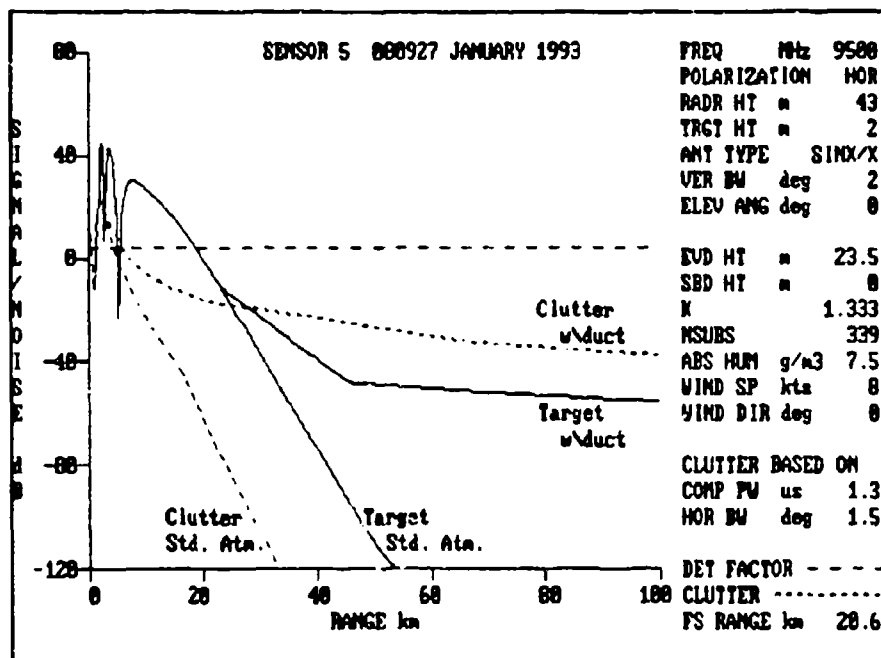


Figure 5.17 EREPS Sea Clutter prediction for Sensor 5 (Case 3).

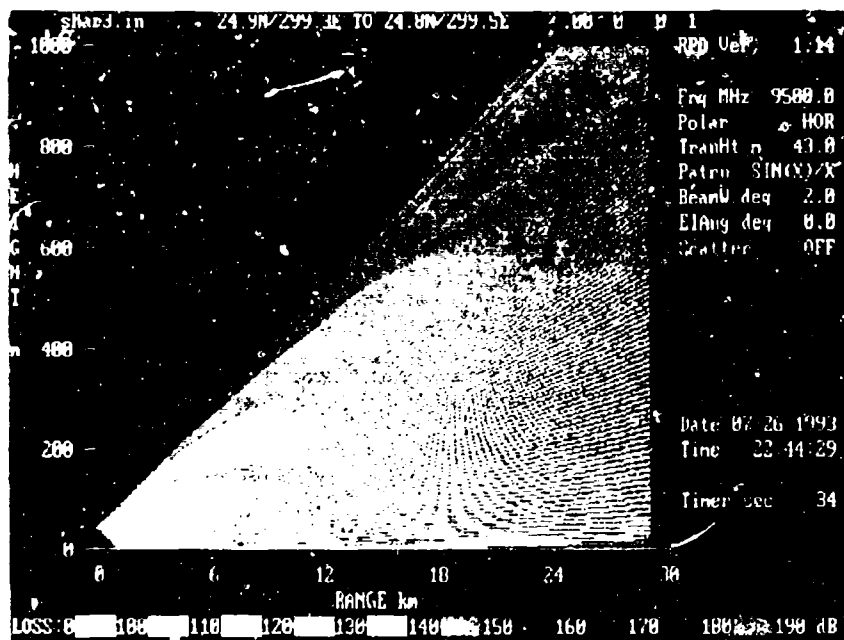


Figure 5.18 RPO Plot of sensor 5 1927L 08 JAN 93
 1000m Seaward Case 1

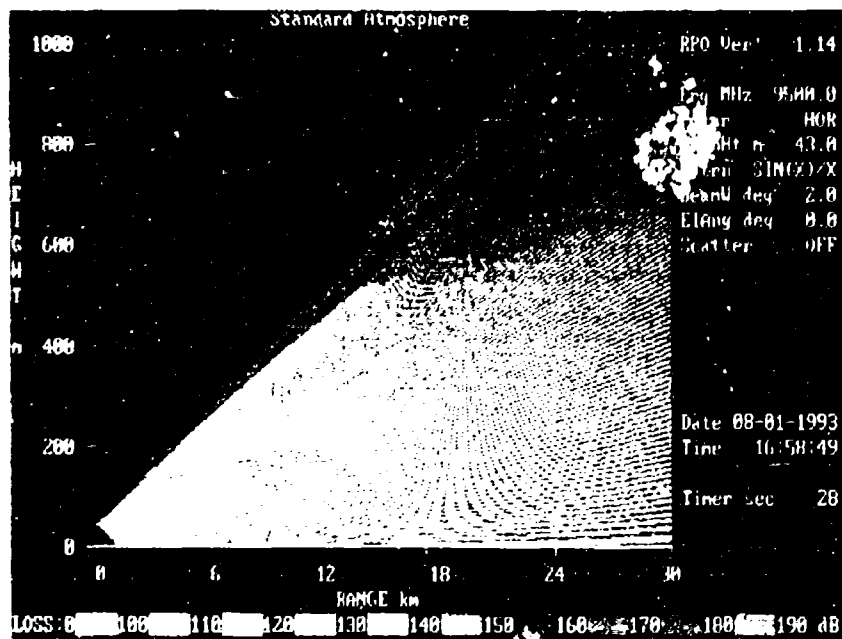


Figure 5.19 RPO Plot of sensor 5 in Standard
 Atmosphere Conditions Case 1

Figure 5.20 appears to support the interpretation of Sensor 4 analysis. Again, looking toward the shore, shown in Figure 5.20, yields better radar performance than looking seaward as depicted in Figure 5.18.

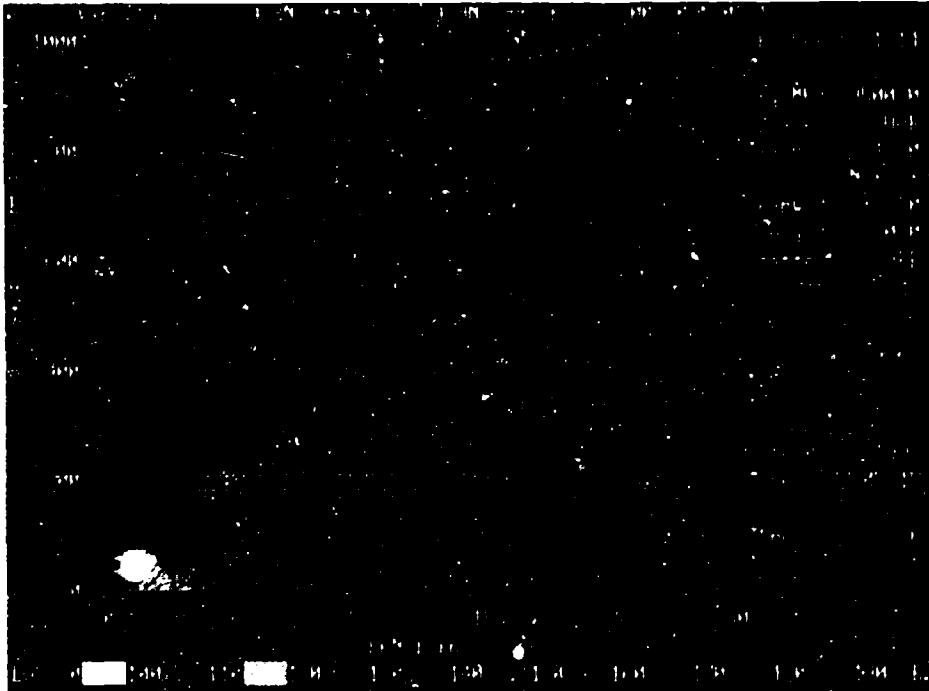


Figure 5.20 RPO Plot of Sensor 5 0927L 08 JAN 93
Looking Towards Shore (Case 3).

3. Case 3 Summary

Interpretation of Sensors 1, 2 and 3 results indicated that the evaporation duct has only minimal affect on EM equipment operating under 3 GHz. However, Sensors 4 and 5 operating at 9.5 GHz experienced extended detection ranges and enhanced sea clutter effects. Although the evaporation duct can yield better ranges usually these are outweighed by sea clutter amplification. Surface-based ducts had no influence in this case since they did not occur.

It was noted in Sensors 4 and 5 EREPS analysis, that an antenna operating just above the evaporation duct experienced a significant increase in detection range as compared to a identical radar operating right below the duct.

It was also found in Sensor 4 and 5 RPO analyses, that radar sensor detection range is enhanced when looking from an area with a weak evaporation duct profile in the direction the duct strengthens.

Although RPO depicts a finer structure of propagation it does not illustrate sea clutter effects. It shows greater radar ranges without qualifying them with sea clutter enhancement. EREPS on the otherhand predicts extended ranges but illustrated that sea clutter would actually dominate to possibly mask any enhancement afforded by the evaporation duct. EREPS was found to be accurate in its predictions of sea clutter, as illustrated in Cases 1 and 2.

VI. SUMMARY AND RECOMMENDATIONS

This thesis examined the assessment of atmospheric influences on surveillance radar performance in littoral zones. Observed influences were sea clutter and extended ranges caused by surface-based and evaporation ducts. The five generic surveillance radar systems parameters used with the atmospheric conditions observed during SHAREM 102, demonstrated how inhomogeneous anomalous propagation can affect low flyer and submarine periscope detection.

Cases 1 and 2 illustrated the need for rawinsonde data to detect strong surface-based ducts undetectable by fixed ship meteorological sensors alone. The surface-based duct had a significant impact on sensor ranges and sea clutter enhancement, as illustrated in the SPANDAR PPI scans, agreeing with prediction by EREPS. It is believed that EREPS is a valuable tool to the ASW tactician in accurately predicting the effects of sea clutter.

Case 3 looked at five generic radar systems of various operating frequencies, polarizations and antenna heights comparing the effect a typical winter Gulf of Oman environmental profile had on their operation and modeling by EREPS and RPO. As described earlier in this thesis, the lower frequency radars, Sensor 1 at 400 MHz and Sensors 2 and 3 at 1.3 GHz were only slightly affected by the presence of an

evaporation duct. However, Sensors 4 and 5 operating performance predictions were profoundly affected. The evaporation duct was responsible for extended ranges in both cases, but the enhancement of sea clutter over powered any gain in detection ranges. Sea clutter in these situations would possibly mask a periscope detection.

Results indicated that detection range is enhanced when looking from an area with a weak evaporation duct profile in the direction the duct strengthens.

It was apparent in the gathering and comparison of SHAREM 102 data, that the validity of ship meteorological measurements of humidity, air temperature, true wind speed and water temperature are questionable. A result of inaccurate atmospheric data is poor prediction of environmental effects on EM/EO systems. This is a critical issue that has to be addressed by the tactician who needs to fully exploit the environment in utilizing his sensors.

Critical requirements exist for accurate, continuous, and real-time measurement of the littoral environment for in situ sensor assessment. For this to be attained various types of sensors must be used; deployable expendable or retrievable bouys or devices, aircraft reporting or even passed on data link within the battle group for input into each ship's environmental/tactical assessment program.

Recommend that future SHAREM exercises examine the radar detection capabilities beyond the visual horizon to exploit the increased ranges provided by strong ducting.

APPENDIX A
SCATTERING AND ABSORPTION FACTORS

The propagation of EM waves is affected by the earth's surface and its atmosphere. If it were not for attenuation and absorption an EM system would have virtually no range limitations other than masking by terrain, objects or interference. The evaporation duct could be considered a lossless wave guide without a horizontal boundary. The rest of this section explores a few of the limiting factors that affect range.

A. Attenuation

Attenuation occurs at both the sea surface and the upper boundary of the lossy wave guide or duct. The evaporation duct's lower boundary is rough and undergoing constant change creating a varying attenuation factor. Attenuation increases as wave height increases and as duct height and frequency of the EM wave decrease.

The non-homogeneous upper boundary allows more EM wave attenuation due to spatial changes in the index of refraction.

B. Absorption

Absorption results from energy being absorbed as heat by atmospheric gases and precipitation and then lost. The density

of the atmosphere decreases with altitude, therefore the affect of absorption also decreases with height. Compared with other factors affecting range absorption is negligible.

C. Antenna Height

More of the EM wave will be trapped for an antenna located lower in the duct than higher or at the upper boundary of the duct. An EM wave reflected at an angle exceeding the critical angle at the top of the duct will also be attenuated. Therefore, to maximize propagation within the duct antenna height must be considered.

APPENDIX B

REFRACTIVITY PREDICTION PROGRAMS

A. Engineer's Refractive Effects Prediction System (EREPS)

EREPS was developed as a set of interrelated programs for scientists and engineers to use in modeling and simulating propagation effects on proposed equipment designs. The different EREPS models take in account diffraction, refraction, tropospheric scatter, sea clutter, evaporation and surfaced-based ducts, water vapor absorption and the interference region of a horizontally homogeneous atmosphere. It has a frequency range of 100 MHz to 20 GHz. EREPS aids the engineer in assessing EM propagation effects of the troposphere on EM systems operating within this region.

EREPS Revision 2.2 was used in preparing this thesis. It consists of five stand-alone IBM/PC compatible programs.

1. PROPR, used to generate a plot of propagation-loss, propagation factor, or radar signal-to-noise ratio (SNR) versus range.
2. PROPH, similar to PROPR except the plot versus height rather than range.
3. COVER, illustrates the area where signal levels are equal to or greater than entered thresholds in a height versus range plot.

4. RAYS, plots a series of rays for entered refractive index profiles in a altitude versus range plot.

5. SDS, displays an annual historical summary of evaporation and surface-based ducts, and other meteorological parameters for 10 by 10 degree squares of the earth's surface. This data can be used in the PROPR, PROPH, and COVER programs.

EREPS limitations are, (Patterson, 1990,p. 87-88)

- PROPR, PROPH and COVER programs are limited to a frequency range of 100 MHz to 20 GHz.
- PROPR, PROPH and COVER models are valid over water only.
- All models assume horizontal homogeneity.
- The diffraction and evaporation duct models are not dependent on the effective earth radius factor (K).
- If a large number of lobes are requested in the optical region, the elevation angles may exceed the small angle assumptions, resulting in null location error.
- A single mode model of propagation is used by all programs for determining evaporation duct height. An error may result for duct heights greater than 30 meters at 3 GHz, 22 meters at 5 GHz, 14 meters at 10 GHz, and 10 meters at 18 GHz. All programs yield acceptable results for ducts between 0 and 40 meters below 2 GHz.
- With the exception of the RAYS program, a single mode empirical model is used to approximate surface-based duct propagation which is used to illustrate the skip zone effect.

- COVER program assumes the direct and sea reflected rays arrive nearly parallel at the receiver or target. This assumption degrades as ranges and altitudes decrease.

1. Georgia Institute of Technology (GIT) Model

The NOSC-modified version of the GIT model is thought to be valid to ± 5 dB. A brief mathematical description is provided taken from (Patterson, 1990, p. 126-131).

Clutter cross-section, in decibels relative to one-square meter

$$\sigma_c = \sigma^o + A_c \quad (1)$$

where

σ^o = average clutter cross-section per unit area, dB

$A_c = 10 \text{ LOG}_{10} [(1000 r \theta_H c \tau_c) / (4 \text{ LOG}_e(2))]$, area of radar resolution cell, dB with

r = range, km

θ_H = radar antenna horizontal beamwidth, radians

c = speed of light, m/sec

τ_c = compressed pulse width, sec.

A radar that is horizontally polarized the equation changes to:

$$\sigma_H^o = 10 \text{ LOG}_{10} (.0000039 \lambda \psi^{0.4} A_1 A_v A_w) \quad (2)$$

where

λ = wavelength

ψ = grazing angle

$A_i = \sigma_p^4 / (1.0 + \sigma_p^4)$, interference factor

$A_u = \exp[0.2 \cos(\phi) (1 - 2.8 \psi) (\lambda + 0.02)^{-0.4}]$, upwind/downwind factor

$A_w = [(1.9425 W_s) / (1 + W_s/15)]^{1.1(\lambda + 0.02)^{-0.4}}$, wind speed factor

$\sigma_p = (14.4 \lambda + 5.5) (\psi h_{avg}) / \lambda$, roughness factor.

For vertically polarized radars with frequencies above 3 GHz the equation takes on a new look:

$$\sigma_v^o = \sigma_H^o - 1.05 \text{LOG}_e(h_{avg} + 0.02) + 1.09 \text{LOG}_e(\lambda) + 1.27 \text{LOG}_e(\psi + 10^{-4}) + 9.70 \quad (3)$$

For vertically polarized radars with frequencies below 3 GHz:

$$\sigma_v^o = \sigma_H^o - 1.73 \text{LOG}_e(h_{avg} + 0.02) + 3.76 \text{LOG}_e(\lambda) + 2.46 \text{LOG}_e(\psi + 10^{-4}) + 22.2 \quad (4)$$

For circularly polarized radars:

$$\sigma_c^o = \sigma_{max}^o - 6 \quad (5)$$

where

σ_{max}^o = the larger of σ_H^o or σ_v^o .

B. Integrated Refractive Effects Prediction System (IREPS)

IREPS was developed at the Naval Ocean Systems Center (NOSC) to provide shipboard environmental data processing and display capability for comprehensive refractive effects assessment of naval surveillance, communications, electronic warfare, and weapons guidance systems. IREPS has been successfully used under operational conditions aboard most carriers to assess and exploit refractive conditions in tactical scenarios. (Patterson, 1990, p. 1)

IREPS was not written to provide performance characteristics for any particular system, rather to give relative system performance assessments for various systems. A large portion of IREPS is concerned with maintaining libraries of existing systems parameters and entering divergent sources of environmental data. Thus, IREPS is not well suited to comparing the performance of two sensors that differ by only one parameter, such as radar pulse length; or to showing relative performance for a given system when only one environmental parameter, such as wind speed or evaporation duct height changes value. (Patterson, 1990, p. 3) For these reasons, three different refractivity programs (EREPS, IREPS, and RPO) will be discussed and used in the course of this thesis.

IREPS has six options available to the user:

1. Select/Enter Environmental Data - The program requires atmospheric data such as temperature, pressure and relative humidity to calculate an M-profile.
2. Propagation Conditions Summary - The summary displays modified refractivity in M-units as a function of altitude and predicted ducts are represented on by shaded areas on a vertical bar to the right of the refractive profile. Also provided are different systems performance characteristics based on calculated profiles.
3. Coverage Display - Illustrates area of coverage for a radar system over a curved-earth and a range versus height plot. Shaded areas show predicted detection ranges. The display also provides system parameters used in the calculations.
4. Loss Display - Energy loss along a path parallel to the earth's surface due to spreading, diffraction, scattering and anomalous propagation. The horizontal dashed lines represent energy levels, or thresholds, necessary for radar detection, radio communication, ESM intercept, or other EM system function.
5. Automode - Produces an automatic generation of any and all IREPS products.
6. Utilities and Editors - This allows the user to print, edit or list data files; enter parameters for radar free space detection range calculations; enter parameters for free space intercept range calculations to determine ESM intercepts;

calculate the evaporation duct height and the surface refractivity in N-units from inputs of surface air temperature, sea surface temperature, surface relative humidity, surface pressure and surface wind velocity; change user data file paths; change default units; and change classification labels. (Patterson, 1990, pp. 5-23)

IREPS has several limitations which must be taken into account while using it for predicting atmospheric propagation.

- Frequency range from 100 MHz to 20 GHz.
- Clutter is not taken into account.
- It assumes horizontal homogeneity.
- Interference effects from sea-reflected rays on airborne systems is not included.
- Atmospheric absorption is not taken into account.
- It does not properly account for the over-the-horizon regions for elevated ducts when the bottom of the duct is just above the antenna height.
- The calculation of free space range does not consider clutter reduction features, such as sensitivity time constant (STC), and moving target indicator (MTI), active electronic countermeasures, or environmental noise. (Patterson, 1990, p. 39)

C. Radio Physics Optics Program (RPO)

RPO uses ray optics and a parabolic wave prediction differential equations to derive and plot propagation loss in

a range versus height format. Unlike IREPS and EREPS, RPO takes into account a horizontally inhomogeneous atmosphere while considering leakage and diffraction effects.

RPO is a hybrid model that uses the complementary strengths of both the ray tracing model and the parabolic equations. Inside a duct, RPO uses the parabolic equation (near horizontal) while outside it uses ray tracing. It allows for user defined polarization methods and accommodates sea surface roughness. With its ability to incorporate different horizontal profiles, RPO is capable of yielding a more accurate picture of the refractive qualities of the atmosphere. However, it does not separate sea clutter from other propagation losses.

LIST OF REFERENCES

Beach, J. B., "Atmospheric Effects on Radio Wave Propagation", *Defence Electronics*, February 1980.

Cook, J., "A sensitivity study of weather data inaccuracies on evaporation duct height algorithms, *Radio Science*, Volume 26, Number 3, pages 731-746, May-June 1991.

Dockery, G. D., *Environmental Support of Cooperative Engagement Capability (CEC) Demonstration Test (DT-I) Phase 3*, Fleet Systems Department, Johns Hopkins University, Applied Physics Laboratory, FS-91-071, November 1991.

Ko, H. and others, *Anomalous Propagation and Radar Coverage Through Inhomogeneous Atmospheres*, AGARD Conference Proceedings 346, 25, 1984.

Morton, J. F., "Antisubmarine Warfare - Still a Priority", an article interview, *Naval Institute, Proceedings*, March 1993.

Patterson, W. L. and others, *Engineer's Refractive Effects Prediction System (EREPS) Revision 2.0*, Naval Ocean Systems Center, San Diego, California, February 1990.

Patterson, W. L., *Integrated Refractive Effects Prediction System (IREPS) User's Manual Revision PC-2.0*, Naval Ocean Systems Center, San Diego, California, August 1990.

Sakkas, C. I., *Information Analysis of Anomalous Propagation Phenomena and Their Effects on EW Systems*, Master's Thesis, Naval Postgraduate School, Monterey, California, June 1984.

Skolnik, M.I., *Introduction to Radar Systems*, 2nd Edition, McGraw-Hill Book Company, 1980.

INITIAL DISTRIBUTION LIST

1. Defense Technical Information Center 2
Cameron Station
Alexandria, Virginia 22304-6145
2. Library, Coa 52 2
Naval Postgraduate School
Monterey, California 93943-5002
3. Director, Space and Electronic Combat Division (N64) 1
Space and Electronic Warfare Directorate
Chief of Naval Operations
Washington, District of Columbia 20350-2000
4. Captain R. Hillyer 1
Commanding Officer PMW-165
Space Warfare Command (SPAWAR)
Arlington, Virginia 22202-5200
5. Captain H. Perry, NAVSEA 62 1
Naval Sea Systems Command
2531 Jefferson Davis Highway
Arlington, Virginia 22242
6. Commander 1
Surface Warfare Development Group Command
2200 Amphibious Drive
Naval Air Base Little Creek
Norfolk, Virginia 23251-2860
7. Johns Hopkins University 1
Applied Physics Laboratory
Johns Hopkins Road
Laurel, Maryland 20723-6009
Attn: G. Dockery, Group F2F
8. Naval Research Laboratory 1
Naval Postgraduate School Annex
Monterey, California 93940-5006
Attn: A. Goroch, Code 400
9. Naval Research Laboratory 1
Naval Postgraduate School Annex
Monterey, California 93940-5006
Attn: M. Pastore, Code 400

- | | |
|---|---|
| 10. Professor K. Davidson
Meteorology Department, Code MR/DS
Naval Postgraduate School
Monterey, California 93943-5002 | 1 |
| 11. Chairman, Electronic Warfare Academic Group
Code EW
Naval Postgraduate School
Monterey, California 93943-5002 | 1 |
| 12. LCDR Kyle M. Craigie
c/o Commanding Officer
VP-30
Naval Air Station
Jacksonville, Florida 32212 | 1 |